Conf-911249--2

CONF-911249--2

DE92 009668

CHARACTERIZATION AND PREDICTION OF SPATIAL VARIABILITY OF UNSATURATED HYDRAULIC PROPERTIES IN A FIELD SOIL: LAS CRUCES, NEW MEXICO

by T.-C. Jim Yeh,

Deborah E. Greenholtz,
Department of Hydrology and Water Resources
The University of Arizona
Tucson, Arizona

Maliha S. Nash,
Department of Crop and Soil Sciences
New Mexico State University
Las Cruces, New Mexico

and

P. J. Wierenga
Department of Soil and Water Science
The University of Arizona
Tucson, Arizona

FG02-91ER61199

DISCLAIMER

ABSTRACT

A 91-m transect was set up in an irrigated field near Las Cruces, New Mexico to investigate the spatial variability of unsaturated soil properties. A total of 455 sampling points were monitored along a grid consisting of 91 stations placed 1 m apart by 5 depths per station. Post-irrigation soil water tension and water content measurements were recorded over 45 days at 11 time periods. The instantaneous profile method was used to estimate the unsaturated hydraulic conductivity at the 455 sampling points. Fifty soil samples were also taken for analyzing sand, silt, and clay content distributions. The spatial and temporal variability of soil water tension and water content were investigated along with the spatial variability of parameters of an unsaturated hydraulic conductivity model. Results of the analysis show that spatial variation in soil water tension and water content is consistent with the soil texture spatial variability. In addition, the spatial distribution of the estimated parameter value of unsaturated hydraulic conductivity reflects the soil texture distribution.

Using the statistics of the estimated hydraulic parameter values, a stochastic soil water tension model was employed to reproduce the variability of observed soil water tension. Although many assumptions were made, the results of the simulation appear promising.

INTRODUCTION

Spatial variability of hydrologic properties of geologic formations has been one of the focuses of hydrologic research during the last decade. Several large-scale field tracer experiments in saturated porous media were conducted in the past few years and a large amount of data were collected to investigate effects of spatial variability (e.g., Sudicky, 1986 and Garabedian et al., 1990). Such carefully collected and extensive field data sets provide the opportunity for testing many theories of flow and solute transport in field-scale problems. Thus, deficiencies of the theories can be identified and improved. For example, Naff et al. (1988) and Dagan (1989) recognize the difficulty of existing three-dimensional macrodispersion theories in reproducing solute plumes at the Borden sand aquifer. Their discussions lead to many speculations of improvements of the theories (Rehfeldt, 1988; Naff et al., 1989; Rajaram and Gelhar, 1991).

Although several stochastic theories on the effect of spatial variability on flow and solute transport in porous media under unsaturated conditions have been developed (e.g., Dagan and Bresler, 1983; Yeh et al., 1985a,b,c; Mantoglou and Gelhar, 1987), only a few large-scale field experiments, where an adequate number of unsaturated hydraulic properties were collected for testing the stochastic theories, have been carried out.

The purpose of this paper is two-fold: first, to describe a field-scale infiltration experiment in a soil, where extensive and detailed hydrologic data were collected and second, to quantitatively assess a soil-water tension variability theory based on a stochastic approach.

MATERIALS AND METHODS

Experimental Field Site

The extensive data analyzed in this study was collected from an experimental plot at the

Leyendecker Plant Science Research Center of New Mexico State University, which is located approximately 14 km southwest of Las Cruces, New Mexico. This is a semi-arid region with an average annual precipitation of 0.23 meters. Rainfall is variable with an average of 52% of the rainfall occurring in July through September. The average maximum temperature is highest in June at 36 degrees C, and lowest in January at 13 degrees C. There is low relative humidity with an average Class A pan evaporation of 2.39 meters per year. The water table is approximately 3 meters deep. (Hendrickx et al., 1984). The soil type at the experimental plot is classified as a Glendale clay loam soil (mixed calcareous thermic family of Typic Torrifluvent) (Hendrickx et al., 1986).

The experimental plot, 93 meters long by 3 meters wide had been prepared for prior experiments by disking in two directions, rototilling to a depth of 0.2 meters, and then levelling using a laser plane. The plot was further smoothed and levelled by hand and enclosed with a 50-centimeter raised soil berm (Nash, 1984).

Sampling stations were set up on the plot 1 meter apart along a 91-meter transect to obtain soil water tension and volumetric water content data. A neutron probe access tube was installed at each station, in the center of the width of the plot, to a depth of 1.5 meters. For each of the 91 stations, five tensiometers were installed across the width of the plot (0.3 meters apart) with their tips at 0.3, 0.6, 0.9, 1.2 and 1.5 meters. A drawing of the experimental plot showing placement of the measuring instruments is provided in Figure 1. Although the five tensiometers associated with each of the 91 stations are not located at the exact site of the access tube, the practical assumption is made that there are only 455 distinct sampling points for measuring soil water content or tension; 91 stations by 5 depths per station. This experimental set-up and the corresponding assumption are based on a standard procedure for measuring soil hydraulic characteristics as described by Hillel et al. (1972). The method requires that a series of tensiometers be installed near the access tube, not greater than 0.3 meters apart and to a depth as great as possible. The tensiometers must be far enough away from the access tube to avoid interfering with the neutron readings (approximately 0.5 meters), yet near enough to monitor the "same" soil mass (Hillel et al., 1972). Nash et al. (1989) maintained that in this particular clay loam soil, the 0.3 meter separation distance is adequate to prevent interference

with neutron probe readings.

Fifty soil samples were taken along the transect at five depths at locations 1, 11, 21, 31, 41, 52, 61, 71, 81, and 91. Sand, silt, and clay contents were determined for these soil samples, using the hydrometer method (Gee and Bauder, 1982).

Volumetric water content was monitored with a neutron probe and moisture meter (CPN Corporation, Howe Road, Martinez, CA, Model 503DR Hydroprobe). As described above, the neutron probe access tubes had been installed vertically into the soil to a depth of 1.5 meters at each of the 91 stations. The neutron probe was lowered into the access tube, and water content readings were collected using standard procedure.

Each actual water content measurement is calculated from the neutron moisture meter reading plus a previously determined calibration curve. The calibration curve plots the relationship between neutron count rate and volumetric water content. The calibration curve is: i = 0.1744 + (Relative Count Ratio) - 0.0347 with 95% confidence limit intervals for an individual predicted value. One calibration curve was used for all sampling locations and soil depths.

Soil water tension was monitored with a system consisting of the 455 installed tensiometers (91 stations by 5 tensiometers per station), and a hand-held pressure transducer with attached hypodermic needle and digital-readout device (Soil Measurement Systems, 7344 North Oracle Road, Tucson, Arizona). This system is based on the design by Marthaler et al. (1983). The needle is injected through a rubber stopper sealing the top of each tensiometer, and the tension measurement is displayed on the readout device. This process can be repeated relatively rapidly until all tension readings have been recorded.

Each tensiometer was made from a porous ceramic cup (5/8 inch outside diameter), PVC pipe (0.5 inch schedule 80), clear plastic tubing (0.5 inch internal diameter; 0.625-inch outside diameter) and a rubber septum stopper. Epoxy Epocast Hardener was used to join the components. The tensiometer was filled with de-aired water leaving only a small volume of air at the top of the tensiometer. After each insertion of the needle, silicon rubber cement was reapplied to the rubber stopper to prevent air leakage.

Before installation of the tensiometers in the experimental plot, each was tested for leakage by submerging it under water and applying up to 1.5 bars of positive pressure. The appearance of bubbles would indicate leakage. The functioning tensiometers were then positioned into holes prepared with a coring tool. Each tensiometer was installed so that 5 centimeters of plastic tubing and rubber septum were aboveground. Before taking measurements, the tensiometers were left to equilibrate with the soil water.

With the tensiometers in place, measurements were taken at the observation times by insertion of the hypodermic needle into the septum stoppers. Readings were recorded directly from the digital read-out device, calibrated in millibars. Then soil water tension values were calculated by subtracting the stem length of the tensiometer from the reading on the meter, in mb or centimeters water.

A drip irrigation system consisting of 12 irrigation lines laid along the length of the plot was installed. Both spacing of the tubes and spacing of drip holes in the tubing was approximately 6 inches. The plot was covered with plastic sheeting to prevent evaporation, and a thin layer of soil to keep the sheeting in place and reduce temperature fluctuations and condensation.

Data were collected at varying irrigation rates in an effort to find the proper rate for reaching steady-state unsaturated flow. Irrigation was not continuous. One-hour pulses of water were applied in six cycles a day (beginning at 10:20 a.m., 2:20 p.m., 6:20 p.m., 10:20 p.m., 2:20 a.m., and 6:20 a.m.). Irrigation began on August 2, 1985 at 1.1 cm/day (900 gal/day). On September 9, the rate was increased to 2.2 cm/day (1800 gal/day). The final irrigation rate of 4.4 cm/day (3600 gal/day) began on October 11 and successfully established the desired steady regime. A steady-state system was assumed when tensiometer readings remained relatively constant at each location over measured time periods. Irrigation ceased on November 25, 1985 after nearly four months of irrigation.

Given this experimental set-up, soil water tension and water content values were measured at each of the 455 sampling stations at 11 different time periods. The times of data collection ranged from 5 hours to 44.25 days after irrigation had stopped. The specific 11 measurement periods are: 0.21 days (5 hours), 0.38 days (9 hours), 1.17, 1.42, 2.25, 3.25, 4.25, 7.25, 11.25, 18.25, and 44.25 days.

Data Preparation: Missing and Outlying Data

The collected water content and soil water tension data sets were reviewed for missing and anomalous wetness and suction values. Missing and suspect data which may have been caused by measurement error, calibration error, malfunction and/or limitations of the measuring instruments, (particularly leaky tensiometers) were discarded before analyses were carried out.

All of the data collected at the first measurement time of 0.21 days (5 hours) were eliminated from this study due to numerous missing data points and positive pressure measurements. For the remaining time periods, both missing values and those identified as unreasonable were estimated as follows. Four hundred fifty five soil moisture characteristic curves (a plot of pairs of θ-ψ data at different times at each sampling location) were constructed, using the neutron probe and tensimeter data. By a visual inspection of the characteristic curves, anomalous values could be identified. Given the water content versus tension relationship for each sampling location, the unreasonable and missing values were then estimated by computer-assisted curve-fitting and/or with a French curve.

A second approach using geostatistics was used to systematically determine unacceptable values (see Greenholtz et al., 1988). Fitted models to the 50 tension semivariograms were used to identify the spatial structure for each depth at a specific time period. Then, tensions could be pinpointed which were inconsistent with the spatial models. After the validation process using hole-by-hole suppression, those values found to have standardized errors between the observed and kriged values greater than a cutoff of 0.9 could be estimated with the kriged value. With 0.9 chosen as the cutoff value, the validation process eliminated or retained values with roughly the same level of selectivity as the visual method.

A final determination of whether a value was unreasonable was based on weighing results of the moisture release curves, the cross-validation of the variogram model, and the level of confidence in each of these. For instance, if a value had a standardized error greater than 0.9 and was out of line on the characteristic curve, that value was estimated. If the characteristic curve did not show a clear relationship, the variogram method for estimation was useful.

Derivation of Hydraulic Conductivity and Pore-Size Distribution Parameters

Hydraulic conductivity values at each location were estimated by the instantaneous profile method (Nielsen et al., 1973) using the water content and soil water tension values available at each location at ten time periods. Assuming that the flux at the plastic-covered soil surface is zero and flow is one-dimensional, the classical instantaneous profile formula for determining unsaturated hydraulic conductivity is:

$$K(\bar{\theta}) = \frac{\int_{o}^{-L} [\theta_{i+1}(z) - \theta_{i}(z)]\, dz}{(t_{i+1} - t_{i})\left(\frac{\partial \bar{h}}{\partial z} + 1\right)} \qquad (1)$$

where K is the unsaturated hydraulic conductivity at the center of a layer between two depths of measurement, Θ is the water content, Θ is the average water content at the location over a time interval, t is a time period, and the subscripts represent two different time values. $\partial h/\partial z$ is the change in time-averaged soil water pressure head with depth. The gradient $\partial h/\partial z$ is estimated with a cubic spline function which fits a smooth curve (continuous first derivative) to the average of the five tension values at time t(i+1) and the five values at t(i) (Nielsen et al., 1973). In the derivation process, the soil surface was treated as having the same water content values as the 0.3-meter depth.

Once the unsaturated hydraulic conductivity values at various moisture contents or suctions were estimated, the following empirical exponential unsaturated hydraulic conductivity model was fit to the data:

$$K(\psi) = K_0 \exp(-\alpha \psi) \qquad (2)$$

where K is hydraulic conductivity, ψ is soil water tension, K_0 is hydraulic conductivity parameter at $\psi = 0$, and α is the pore-size distribution parameter. When plotted on semilog paper with tension on the linear x-axis, K_0 is the intercept and α is the slope.

RESULTS AND DISCUSSION

Soil Texture

Figures 2a, b, and c illustrate the spatial distribution of percentage of sand, silt, and clay content along the profile, respectively. The percentage of sand content throughout the profile increases with depth with an anomaly near the upper-center portion of the profile. On the other hand, silt content tends to decrease with depth. Similar to the silt content distribution, the clay content decreases with depth. However, soils with high clay content values were found near the region between depths 60-120 cm and locations 41 -81. Statistical analysis of sand, silt, and clay contents was carried out for data collected at the depth 30 cm (Greenholtz, 1991). However, no statistical analysis was conducted for the entire soil profile.

Volumetric Water Content Profiles

Contour plots constructed for water content for selected times (0.38 days, 11.25 days, and 44.25 days) are displayed in Figure 3a, b, and c. These plots were made using a contouring program , which uses the inverse distance squared method to construct the contours. Note that the contour program smooths contours and deletes extreme values.

In this case kriged maps were not made because there were not enough data points to define an experimental semivariogram for the vertical direction, and because of the disparity between observation intervals along the horizontal and vertical scales. The plots show cross-sections, with the x-axis corresponding to transect locations, and the y-axis corresponding to depth from 0.3 meters (top of plot) to 1.5 meters (bottom of plot). Over the time periods, the water content value for any particular point on the plot decreases. It is evident from the plots that the highest water contents are found at the upper depths towards the center of the transect. The lowest water contents are found at the lowermost depth, which has greater uniformity of water content values. The most rapid changes in water content with depth (i.e. plotted lines are close together) are found at the middle depths, particularly towards the center of the transect. The change to a lower gradient at approximately 1.2 meters is interpreted as a change in texture. Over time, the contour plots retain the same general shape. Therefore, the distribution of water content remains similar over the measurement times.

Mean Water Content

Because the soil was observed during drying, a decrease in water content is expected over time. Over the observed time periods, the mean water content values do decrease for each depth. These means range from 0.382 cm^3/cm^3 (at time 0.38 days) for depth 0.6 meters to 0.116 cm^3/cm^3 (at time 44.25 days) at the lowest depth. Over the 44 days, the change in mean water content is: 0.069 cm^3/cm^3 (1.2-meter depth) > 0.060 (0.9-meter depth) > 0.057 (1.5-meter depth) > 0.048 (0.6-meter depth) > 0.033 (0.3-meter depth). Plots of the mean water content values over time for the five depths are shown in Figure 4. It is evident that the decrease of water content over time is most rapid for the earliest times after ceasing of irrigation. The plots then tend to level off (i.e. slowing of the drying rate), particularly at the upper depths. This slowing of the drying rate may result from the drop in unsaturated hydraulic conductivity as water content decreases over time.

For any given time period, the highest mean water contents are found at the two uppermost depths. Thereafter, water content decreases with depth. The mean water content values at each depth (averaged over the ten times) follow this same trend of a lowering of water content with depth: 0.363 cm^3/cm^3 (0.6-meter depth) > 0.355 (0.3-meter depth) > 0.284 (0.9-meter depth) > 0.170 (1.2-meter depth) > 0.153 (1.5-meter depth). From inspection of Figure 4, plots of the mean water content values over time for the five depths, we again see that the 0.3- and 0.6-meter depths have the highest mean water contents but seem to level off slightly more than the lower depths over time. This shows more constant water content values with a slower drying rate at later times. For the lower depths, there is greater change in water content over time, the drying rate is more rapid, and the drying rate remains more constant over time.

These results of higher mean water contents at the upper depths and lower mean water contents at the lower depths associated with more rapid drying are, again, consistent with the soil texture data. The lower depths have coarser texture associated with lower retention and more rapid transmission of water.

Variation of Water Content

Plots of variance of water content over time for the five depths are illustrated in Figure 5. Depths 0.6 and 0.9 meters show a clear increase of variance over the drying period, depth 0.3 meters levels off after approximately 11 days, and the lower two depths show a decrease of variance after 8 to 11 days. The middle three depths have higher variance of water content values for any given time period, and the uppermost and lowermost depths have lower variation. (For all time periods, depth 0.9 meters has the highest variance, and depth 0.3 meters has the lowest.) The depths which exhibit lower variances (i.e depths 0.3 and 1.5 meters, and to a lesser extent, 1.2 meters) show the most uniform water content versus location plots across the transect and over the time periods.

At each of the five depths it is found that as mean water content increases, the variance of water content clearly decreases for the 0.3-, 0.6-, and 0.9-meter depths. No clear trend is evident for the 1.2-meter depth. For the 1.5-meter depth, there is an apparent increase in variance as water content increases. The steepest slope (i.e. the greatest change of variance with increased water content) is found for the 0.6 > 0.9 > 0.3-meter depth.

In order to standardize the variances, coefficients of variation were computed (i.e. standard deviation divided by the mean). Coefficients of variation are preferable for comparing distributions with differing means. At all depths, the coefficients of variation for water content clearly increase over the ten time periods as the soil dries out. Variability of water content ranges from 6-9% in the uppermost depth to 26-45% in the lower two depths. The increases of the coefficients of variation over time are consistent with the theory that variability should increase as a soil dries. The slopes for the two uppermost depths are the least steep and level off more, showing less variability at these depths, particularly for later times. The 0.3-meter depth, which has a rather uniform water content distribution along the transect shows low variability and little change over time.

At any given time period, there are higher coefficients of variation with increased depth (with the exception that depth 1.2 meters had a higher value than depth 1.5 meters). The mean coefficient of variation averaged over the ten time periods similarly increases with depth ranging from 7% at the 0.3-meter depth to 37% at the 1.2-meter depth. The higher coefficients of variation of water content found at the lower sandy depths may be related to textural or pore-size differences across the transect.

Note that the water content versus location plots seem to show less variability for these lower depths. However, because the mean water content value is much lower for the lower depths, the coefficient of variation calculated relative to the mean is high.

Figure 6 shows the plot of the coefficient of variation for water content versus the mean water content at the five depths. The coefficient of variation for water content increases as the mean water content decreases. Similar results were also reported by Herkelrath et al., 1991. The slopes for depths 0.6, 0.9, and 1.2 meters are apparently similar. The 1.5-meter depth slope is somewhat less steep, and the 0.3-meter depth has the least steep slope. Thus, as water content changes, the variation is least affected for the upper and lower depth.

Histograms were constructed on the raw data for the five depths at each time to visually inspect the water content frequency distributions. Various degrees of normality are exhibited with left or right skewness evident in several histograms. Histograms are approximately uniform for the 0.3-meter depth, tend to be skewed left for the 0.6-meter depth, tend to be bimodal for the 0.9-meter depth, are skewed right for the 1.2-meter depth, and are approximately normal for the 1.5-meter depth.

Soil Water Tension

Contour plots of tension for selected times (0.38, 11.25 and 44.25 days) are shown in Figure 7. The plots show cross-sections, with the x-axis corresponding to transect locations, and the y-axis corresponding to depth from 0.3 meters (top of plot) to 1.5 meters (bottom of plot). Over the time periods, the tension value for any particular point on the plot increases. The highest tensions are found towards the ends of the transect. These high tensions are found at the middle depths for time 0.38 days, and extend to the upper-middle depths for the later times. The lowest tensions are found towards the middle of the transect, and extend from the mid-lower depths at time 0.38 days to the upper-middle depths at later times. Thus, the area of lowest tension found in the middle of the transect shifts from the lower depths to the mid-upper depths over the 44 days. The most rapid differences in tension values across the transect (i.e. plotted lines are close together) are found

approximately near locations 25 and 75. Over time, the graphs retain the same general shape, but not as strongly as for water content.

Contour plots of total hydraulic head for selected times (0.38 and 44.25 days) are displayed in Figure 8. Assuming isotropic porous media, lines drawn perpendicular to the equal head contours show the direction of water flow. For any given point on the plot at 0.38 days, a lower head value (i.e. higher negative numbers) is found for 44.25 days. The contour plot at 0.38 days shows less variability of head values across the transect for middle to upper depths, whereas more pronounced differences in head values are apparent across the transect at 44.25 days.

For the lowermost depth, there seems to be less variability across the transect at 44.25 days. The lowest head values are found at the lower depths for 0.38 days, and extend to the lower-middle depths at 44.25 days, consistent with downward drainage. Flow is not exactly vertical, as assumed in the instantaneous profile method. Yet, the basic downward trend of flow is apparent. There may be some lateral flow (i.e. leaving the plane of the grid), indicated by the intersection of flow lines at time 0.38 days near locations 15 and 80. Highest head gradients are found in the upper-middle depths where head lines are closest together, which may correspond to lower hydraulic conductivity. The lower sandy depths have smaller head gradients and higher hydraulic conductivity. The gradient at the upper-middle depth is similar for the two plotted time periods. The highest gradients found are 0.75 cm/cm at time 0.38 days and 0.68 cm/cm at 44.25 days. There is some similarity between water content and total head contour maps. The wettest area is central and towards the upper soil depths, and head maps show water flowing from that area.

Mean Tension

Because the soil was observed during drying, an increase in suction would be expected over time. For all depths, the expected increase of mean tension clearly did occur over time as shown in Figure 9 where plots of mean tension versus time for the five depths are illustrated. Mean tension values range from 35.1 cm water (at depth 0.6 meters and time 0.38 days) to 99.4 cm water (at depth 0.3 meters and time 44.25 days). Over the 44 days, the mean tension values increased the most at the

upper depths and the least at the lower depths. Specifically, the mean changes are 62.8 (0.3-meter depth) > 53.1 (0.6-meter depth) > 38.6 (0.9-meter depth) > 30.8 (1.2-meter depth) > 21.4 (1.5-meter depth). In Figure 9, the plotted lines for the upper depths are steeper, showing a more rapid increase of mean tension over time. The plotted lines for the lower depths (particularly for depth 1.5 meters) are less steep, and level off over time (i.e. little change in mean tension over time). Therefore, at the sandy lower depth, tension rapidly increases after ceasing of irrigation, but later remains nearly constant over time. Water passes through this coarse-textured layer, which has high hydraulic conductivity and low retention of water. This same result was reported by Nash (1984) on the same soil in a flooded plot experiment.

Mean tension trends with depth are not clear, but depend on the given time period (Figure 9). At early times, the mid to lower depths tend to have the highest tensions. At later times, the upper to mid depths have the highest tensions. The following trend is found for the five mean tension values (averaged over the ten times): 66.01 cm (1.2-meter depth) > 65 95 (0.9-meter depth) > 64.69 (0.3-meter depth) > 55.97 (0.6-meter depth) > 52.36 (1.5-meter depth).

Variation of Tension

In the past most researchers have found greater variation of soil water tension and water content as a soil dries. As seen in Figure 10, an increase of tension variance over time is demonstrated for depths 0.3 and 0.6 m; the lower depths suggest a relatively constant or possibly decreasing trend. As evident in the graphs, the lower three depths exhibit little change in variance over time.

The highest variance for any given time is found at depth 0.6 meters > 0.9 meters > 0.3 meters > 1.2 meters > 1.5 meters. Depths 1.2 and 1.5 meters, which are uniformly sandy, have the lowest variances. As evident in this plot, variances at the lower three depths remain relatively constant over time. For depths 0.3 and 0.6 meters, there is a greater change in variance as the soil dries. These depths have higher percentages of silt and clay than the lower depths (Figure 2a, b, and c).

A plot of the variance of tension versus mean soil water tension for each of the five depths shows, that, as the mean soil water tension increases, the variance of soil water tension generally

increases at depths 0.3 and 0.6 meters. These two upper depths exhibit the steepest slopes (i.e. the greatest change of variance with increased water content). Variances at the lower three depths remain approximately constant or show slight decreasing trends.

As evident in Figure 10 (a plot of coefficients of variation for tension over time at the five depths), a generally decreasing trend of the tension coefficients of variation over time is observed at each of the five depths. Plotted lines for the lower two depths decrease and then level off at approximately 18 days. Thereafter, the variation remains constant for these depths. Depth 0.6 meter has the steepest slope, and shows the decrease of variation continuing even at 44 days of draining. At any given time period, the highest coefficients of variation for tension are found for the middle 0.6- and 0.9- meter depths (ranging from 31 to 98%), and the lowest coefficients are found for the lower 1.2-meter and 1.5-meter depths (ranging from 11 to 30%).

Coefficients of variation of tension decrease over time for the five depths. The high coefficients of variation observed at the earliest time periods may be due to nonuniform infiltration of water into the soil. At later times, the water has had more chance to redistribute resulting in less variability (Nash, 1984). As evident in this plot, the highest coefficients of variation for any given time are found at depth 0.6 meters > 0.9 meters > 0.3 meters > 1.5 meters > 1.2 meters. Plots for the lower two depths level off the most, showing the least change in variation over time. Again, the soil at this depth is uniformly sandy.

For the upper depths, tension tends to have higher coefficients of variation than water content. For the lower sandy depths, water content exhibits the highest coefficients of variation and tension exhibits the lowest coefficients of variation. This is consistent with Nash's result in a flooded plot experiment at the same site (1984, pp. 126-127). The soil moisture characteristic curve for a coarse-textured soil may help to explain this relationship. In a sandy soil, most of the pores are relatively large. The pores drain readily with very little change in suction. Therefore, there can be a large change in water content with large coefficients of variation for water content, associated with a small change in tension and small coefficients of variation for tension. Explanation based on a mathematic model is given in the later section. A plot of the coefficient of variation for tension versus the mean soil

water tension is displayed in Figure 11.

Shapes of histograms constructed on the raw data varied with time and depth. Both right and left skewness was present. Histograms are skewed right for the 0.3-meter and 0.6-meter depth, skewed left or possibly bimodal for the 0.9-meter depth, approximately normal for the 1.2-meter depth, and skewed left for the 1.5-meter depth.

Hydraulic Conductivity Parameters: K_0 and α

As described earlier, hydraulic conductivity (K_0) and pore-size distribution parameter (α) were derived from a linear regression of natural log of unsaturated hydraulic conductivity on tension using the exponential unsaturated hydraulic conductivity model (Eq. 2). As a result, the model may not represent the actual K-ψ relationship of some soils over the entire range of ψ values, but the range where the model is fitted. In this field experiment, most of θ and ψ data collected fall in a range of tensions from 30 to 100 cm of water. It is likely that the estimated K_0 may not correspond to actual saturated hydraulic conductivity values of the soil but the intercept extrapolating from the linear lnK-ψ model fitted to the range of ψ values. Similarly, the estimated α values may not represent the rate of reduction in K over the entire range of ψ values. Consequently, the derived K_0 and α values were found to have excessively large means, variances, and coefficients of variation at each depth (Table 1). The horizontal correlation scales resulting from variogram analyses of the data of K_0 are 5, 16, 35, 7, and 5 meters for depths 0.3, 0.6, 0.9, 1.2, and 1.5 meters, respectively. The corresponding values for the α parameter at these depths are 6, 10, 8, 11, and 5 meters (Greenhlotz, 1990).

Contour plots of K_0 and α distributions are illustrated in Figures 12a and b, respectively. The highest α values are found at the lower depths on the ends of the transect, particularly at high-numbered locations. These are the same areas where the highest K_0 values are found. The general increase of K_0 and α values with depth is consistent with the change to coarser texture with depth (see Figures 2a, b, and c).

Stochastic Model

Yeh et al. (1985 a,b, and c) developed a mathematical model for quantifying spatial variability of soil water tension in field soils, using a stochastic analysis. Based on their analysis, the coefficient of variation of soil water tension in media with three-dimensional, stationary random K_0 and α fields (assuming they are uncorrelated) and under unit-mean-gradient flow condition can be expressed as

$$CV_\psi = \frac{\sigma_\psi}{H} = \left[\frac{(\sigma_f^2 + \sigma_\alpha^2 H^2)\lambda^2}{H^2 A\lambda(1+A\lambda)}\right]^{1/2} \qquad (3)$$

where σ_ψ, σ^2_f, and σ^2_α denote the standard deviation of soil water tension, and the variance of natural log of K_0 and α, respectively. The mean soil water tension is represented by H; the mean α parameter value is donated by A; the vertical correlation scale of the two parameters is λ. Note that the model assumes the horizontal correlation scales are much larger than the vertical (i.e., a perfectly stratified soil formation).

According to this model, the variance of soil water tension will increase as the mean soil water tension increases. Yeh (1989) also explained the phenomenon that for soils with correlated K_0 and α fields, the variance of soil water tension will decrease first and then increase as soils dry out. That is, the variance of soil water tension depends upon the mean soil water tension.

Such a concept of mean-dependent variability of soil water tension was tested by Yeh and Harvey (1990), using soil column experiments. The agreement between results from observations and predictions using the stochastic model is found reasonably good. Qualitative confirmation of the concept of the mean-dependent variability of soil water tension are provided by recent field observations (e.g., Yeh et al., 1986; Herkelrath et al., 1991). However, a quantitative evaluation of the model requires many measurements of unsaturated hydraulic conductivity values of the field soil. The extensive data collected during this field experiment provide the first opportunity for testing the mean-dependent tension variability hypothesis and the stochastic model for field soils in a quantitative manner.

To carry out this test, we assume that there are five distinct layers, corresponding to the five

depths. In addition, mean soil water tension within each layer during each sampling time is assumed to be uniform over the thickness of the layer and the flow is steady. With these assumptions, Table 1 provides all the parameter values required for the model, except the vertical correlation scale due to insufficient number of samples in the vertical direction. To circumvent the difficulty in obtaining the vertical correlation scale, the stochastic model (Eq. 3) was fitted to the observed data by adjusting the value of the vertical correlation scale. Figure 11 shows the fitted theoretical and observed CV and H relationships. The vertical correlation scales determined from the best-fit stochastic model are 0.024, 0.087, 0.02, 0.0017, and 0.0021 meters for depths 0.3, 0.6, 0.9, 1.2, and 1.5 meters, respectively. Although the precision of values of the correlation scales can not be verified, the general trend of the values seems consistent with soil texture data: fine-textured material tends to have a long correlation scale and coarse-textured material a short correlation scale.

The agreement between the calculated and observed coefficient of variation and mean soil water tension relationships is reasonably good but we must emphasize the fact that it is a result of regression analysis. The predictive capability of the stochastic model still remains unknown. However, it is interesting to note that the model predicts the general trend of the relationship very well. In other words, the model structure, derived from physically correct flow equations, appears sound, regardless of many simplified assumptions used in the derivation.

The stochastic model also provides a way for explaining the phenomenon that the CV of moisture content increases as the mean water content decreases. If a simple linear relationship is assumed for the moisture release curve of the soil, i.e.,

$$\theta = c\psi + d \tag{4}$$

where θ is the moisture content. Both θ and ψ are random quantities. In addition, c and d also can vary spatially and thus are taken to be random variables. The mean and variance of θ can be approximated by linearizing the $c\psi$ term in (4) and ignoring the correlation between ψ and c or d. That is,

$$\Theta = CH \tag{5}$$

for the relationship between the mean water content Θ and mean soil-water tension, and the associated variance is

$$\sigma_\theta^2 = C^2\sigma_\psi^2 + H^2\sigma_c^2 + \sigma_d^2 + 2H\ cov(c,d) \tag{6}$$

If c and d are assumed to be deterministic variables and use (3), then the CV of water content can be expressed as

$$CV_\theta = \frac{\sigma_\theta}{\Theta} = \sqrt{\frac{(C^2\sigma_f^2 + \sigma_d^2\,\Theta^2)\lambda^2}{\Theta^2 A\lambda(1 + A\lambda)}} \tag{7}$$

According to this equation the CV in water content will grow as the soil dries out. Note that this equation does not predict the linear trend as shown in Figure 6. This may be attributed to misrepresentation of the water release curve in the field by the linear model (4). Other nonlinear relationships can be used for the curve but the analysis may be complex.

Practical applications of the stochastic tension model tested in this paper may include estimation of uncertainty due to spatial variability. As a common practice in modeling moisture movement in unsaturated zone, one is likely to assume the medium is homogeneous and predict the mean flow field (e.g., Yeh et al., 1985a, b, and c; Mantoglou and Gelhar, 1987 a,b, and c; Yeh, 1989, Yeh and Harvey, 1990; and Polmann et al., 1991). To estimate deviations from the mean (uncertainties) resulting from the unmodeled heterogeneity, the stochastic tension model becomes a useful tool (a good example is given in Polmann et al., 1991). Indeed, if tension distribution can be

assumed normally distributed, this estimate of uncertainty may provide a simple way to answer a practical question commonly raised by farmers: what percentage of a field is under-irrigated for a given water application rate?

Furthermore, unlike in the saturated flow, where hydraulic head variation is relatively small (Gelhar, 1986), the variance of soil water tension is generally large and varies with the mean tension. Consequently, the variability of tension can be easily monitored with a large number of tensiometers as demonstrated in this paper. If some estimates of the variance of ln K_0 and α parameters are available, the stochastic tension model may provide a simply means to estimate correlation scales. Obviously, more field experiments are needed to rigorously validate the model and the approach.

CONCLUSIONS

Extensive soil water content and tension data in a soil profile were collected at various time intervals during drainage. Soil samples were taken for analyzing sand, silt, and clay contents. Soil water content and tension data were analyzed to investigate the spatial variability. Several conclusions are drawn from the result of this investigation. They are summarized as follows:

1) In spite of uncertainties in measurements, the general behavior of the observed soil water content and tension along the profile is consistent with observed soil texture data.

2) The instantaneous profile method for determining unsaturated hydraulic properties seems adequate to depict the spatial variability of unsaturated soil properties, regardless of its simplicity.

3) K_0 and α values obtained by fitting lnK-ψ model to K-ψ data estimated from the instantaneous profile method may not reflect accurate saturated hydraulic conductivity values, but the "bulk" spatial distributions of both K_0 and α values are in a good agreement with soil texture distributions.

4) Observed spatial variability of soil water content and tension qualitatively supports the validity of the stochastic tension model developed by Yeh et al. (1985 a,b, and c) although more carefully planed field experiments are obviously needed.

ACKNOWLEDGEMENT

This research is supported by a grant from Ecological Research Division, ER-75, Office of Health & Environmental Research, Office of Energy Research, Department of Energy under the contract, DE-FG02-91ER61199.

REFERENCES

Dagan G. and E. Bresler, Unsaturated flow in spatially variable fields, 1, Derivation of models of infiltration and redistribution, *Water Resour. Res.*, 19(2), 1983.

Dagan, G. Comment on "A note on the recent natural gradient tracer test at the Borden site" by R.L. Naff, T.-C. J. Yeh, and M. W. Kemblowski, *Water Resour. Res.*, 25(12), 2521-2522, 1989.

Hendrickx, J.M.H., P.J. Wierenga, and M.S. Nash, Variability of soil water tension and soil water content. Presented at 1984 Winter Meeting of American Society of Agricultural Engineers, 1984.

Hendrickx, J.M.H., P.J. Wierenga, M.S. Nash, and D.R. Nielsen, Boundary location from texture, soil moisture, and infiltration data. *Soil Sci. Soc. Am. J.* 50, 1515-1520, 1986.

Herkelrath, W.N., S.P. Hamburg, and F. Murphy, 'Automatic, real-time monitoring of soil moisture in a remote field area with time domain reflectometry', *Water Resour. Res.*, 27(5), 857-864, 1991.

Hillel, D.V., D. Krentos, and Y. Stylianou, Procedure and test of an internal drainage method for measuring soil hydraulic characteristics in situ. *Soil Sci.* 114(5), 395-400, 1972.

Garabedian, S.P., D. R. LeBlanc, L. W. Gelhar, and Michael A. Celia, Large-scale natural gradient tracer test in sand and gravel, Cape Code, Massachusetts, 2. Analysis of spatial moments for a nonreactive tracer, *Water Resour. Res.*, 27(5), 911-924, 1991.

Gee G. W. and W. Bauder, Particle-size analysis, A. Klute (ed.), in: *Methods of Soil Analysis*, Part I, Physical and mineralogical methods, 2nd edition, ASA Inc. Madision, Wisconsin, p 383-411, 1982.

Gelhar L.W., Stochastic subsurface hydrology from theory to applications, *Water Resour. Res.*, 22(9), 135S-145S, 1986.

Greenholtz, D.E., Spatial variability of hydrologic properties in an irrigated soil, Master's thesis, Dept. of Hydr. and Water Resour., The Univ. of Arizona, Tucson Arizona, 1990.

Greenholtz, D.E., T.-C. J. Yeh, M. B. Nash, P. J. Wierenga, Geostatistical analysis of soil hydrologic properties in a field plot, *Jour. of Cont. Hydro.*, 3, 227-250, 1988.

Mantoglou, A., and L.W. Gelhar, Stochastic modeling of large-scale transient unsaturated flow systems. *Water Resour. Res.* 23(1), 37-46, 1987a.

Mantoglou, A., and L.W. Gelhar, Capillary head tension variance, mean soil moisture content, and effective soil moisture capacity of transient unsaturated flow in stratified soils. *Water Resour. Res.* 23(1), 47-56, 1987b.

Mantoglou, A., and L.W. Gelhar, Effective hydraulic conductivity of transient unsaturated flow in stratified soils. *Water Resour. Res.*, 23(1), 57-68, 1987c.

Marthaler, H.P., W. Vogelsanger, F. Richard, and P.J. Wierenga, A pressure transducer for field tensiometers. *Soil Sci. Soc. Am. J.* 47, 624-627, 1983.

Naff, R.L., T.-C. J. Yeh, and M. W. Kemblowski, A note on the recent natural gradient tracer test at the Borden site, *Water Resour. Res.*, 24(12), 2099-2103, 1988.

Naff, R.L., T.-C. J. Yeh, and M.W. Kemblowski, Reply, *Water Resour. Res.*, 25(12), 2523-2525, 1989.

Nash, M.S.B., Variability in soil water tension, water content and drainage rate along a line transect. Master's thesis. New Mexico State University, Las Cruces, NM, 1984.

Nash, M.S., P.J. Wierenga, and A. Butler-Nance, Variation in tension, water content, and drainage rate along a 91-m transect. *Soil Sci.* 148(2), 94-101, 1989.

Nielsen, D.R., J.W. Biggar, and K.T. Erh, Spatial variability of field-measured soil-water properties. *Hilgardia.* 42(7), 215-259, 1973.

Polmann D. J., D. McLaughlin, S. L. Luis, L. W. Gelhar, L.W. Gelhar, and R. Ababou, Stochastic modeling of large-scale flow in heterogeneous unsaturated soils, *Water Resour. Res.*, 27(7), 1447-1458, 1991.

Rajaram H. and L. W. Gelhar, 'Three-dimensional spatial moments analysis of the Borden tracer test', *Water Resour. Res.*, 27(6), 1239-1251, 1991.

Rehfeldt, K. R. Prediction of macrodispersivity in heterogeneous aquifers, Ph.D. dissertation, Mass. Inst. of Technol., Cambridge, 1988.

Sudicky, E. A. A natural gradient experiment in a sand aquifer: Spatial variability of hydraulic conductivity and its role in the dispersion process, *Water Resour. Res.*, 22(13), 1447-1458, 1991.

Yeh, T.-C.J., L.W. Gelhar, and A.L. Gutjahr, Stochastic analysis of unsaturated flow in heterogeneous soils. 1. Statistically isotropic media. *Water Resour. Res.* 21(4), 447-456, 1985a.

Yeh, T.-C.J., L.W. Gelhar, and A.L. Gutjahr, Stochastic analysis of unsaturated flow in heterogeneous soils. 2. Statistically anisotropic media. *Water Resour. Res.* 21(4), 457-464, 1985b.

Yeh, T.-C.J., L.W. Gelhar, and A.L. Gutjahr, Stochastic analysis of unsaturated flow in heterogeneous soils. 3. Observations and applications. *Water Resour. Res.* 21(4), 465-471, 1985c.

Yeh, T.-C.J., L.W. Gelhar, and P.J. Wierenga, Observations of spatial variability of soil-water pressure in a field soil. *Soil Sci.* 142(1), 7-12, 1986.

Yeh, T.-C.J., One-dimensional steady state infiltration in heterogeneous soils. *Water Resour. Res.* 25(10), 2149-2158, 1989.

Yeh, T.-C.J. and D. J. Harvey, Effective hydraulic conductivity of layered sands, *Water Resour. Res.*, 26(6), 1271-1279, 1990.

Table

Table 1. Means, variances, and coefficients of variations of estimated $\ln K_0$ and α values at each depth

Figure captions

Figure 1. Drawing of the experimental plot showing placement of neutron probes and tensiometers.

Figure 2. Spatial distribution of percentage of a) sand, b) silt, and c) clay contents along the profile.

Figure 3. Contour plots of water content for a) 0.38 days, b) 11.25 days, and c) 44.25 days.

Figure 4. Mean water content over time for the five depths.

Figure 5. Variance of water content over time for the five depths.

Figure 6. Coefficient of variation for water content versus mean water content.

Figure 7. Contour plots of soil-water tension for a) 0.38 days, b) 11.25 days, and c) 44.25 days.

Figure 8. Contour plots of total hydraulic head for a) 0.38 days and b) 44.25 days.

Figure 9. Mean soil-water tension over time for the five depths.

Figure 10. Variance of soil-water tension over time for the five depths.

Figure 11. Coefficient of variation for soil-water tension versus mean soil-water tension.
solid line - stochastic model

Figure 12. Contour plots of a) natural log of saturated hydraulic conductivity and b) pore-size distribution parameter.

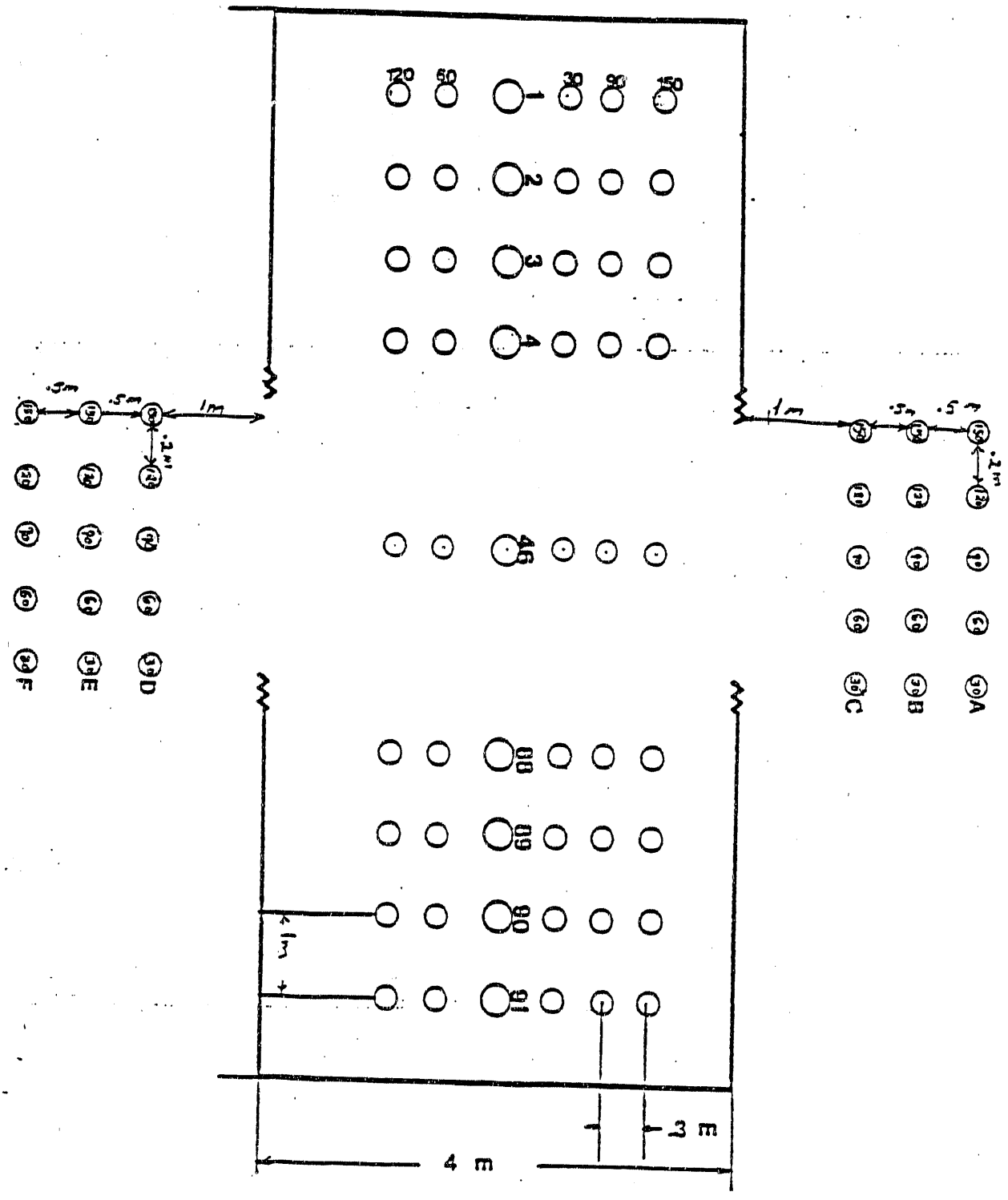

Figure 1 Drawing of the experimental plot showing placement of neutron probes and tensiometers

Table 1. Basic statistics for saturated hydraulic conductivity and pore-size distribution parameter derived using the final data set

	KSAT	ALPHA	LNKSAT
DEPTH 0.3 METERS			
MEAN	1.44E+05	0.095	2.29
MINIMUM	1.40E-05	-0.200	-11.12
MAXIMUM	1.24E+07	0.397	16.33
ST. DEV.	1.29E+06	0.068	3.45
VARIANCE	1.70E+12	0.005	11.88
COEFF. VAR.	8.98E+02	71.8	150.2
DEPTH 0.6 METERS			
MEAN	8.15E+04	0.087	1.66
MINIMUM	7.63E-02	0.027	-2.57
MAXIMUM	6.09E+06	0.204	15.62
ST. DEV.	6.46E+05	0.040	3.58
VARIANCE	4.20E+11	0.002	12.84
COEFF. VAR.	7.93E+02	45.7	215.8
DEPTH 0.9 METERS			
MEAN	7.80E+13	0.127	5.87
MINIMUM	1.67E-01	0.016	-1.79
MAXIMUM	7.10E+15	0.366	36.50
ST. DEV.	7.40E+14	0.063	6.44
VARIANCE	5.50E+29	0.004	41.52
COEFF. VAR.	9.49E+02	49.5	109.9
DEPTH 1.2 METERS			
MEAN	1.20E+17	0.146	8.35
MINIMUM	1.49E+00	0.049	0.40
MAXIMUM	1.10E+19	0.531	43.84
ST. DEV.	1.10E+18	0.071	5.92
VARIANCE	1.30E+36	0.005	35.07
COEFF. VAR.	9.49E+02	48.7	70.9
DEPTH 1.5 METERS			
MEAN	3.20E+17	0.195	9.11
MINIMUM	2.33E-04	0.022	-8.36
MAXIMUM	2.90E+19	0.758	44.81
ST. DEV.	3.00E+18	0.133	8.20
VARIANCE	9.00E+36	0.018	67.29
COEFF. VAR.	9.47E+02	68.5	90.0

KSAT = Saturated hydraulic conductivity parameter (cm/day)
ALPHA = Pore-size distribution parameter (1/cm)
LNKSAT = Natural log of KSAT

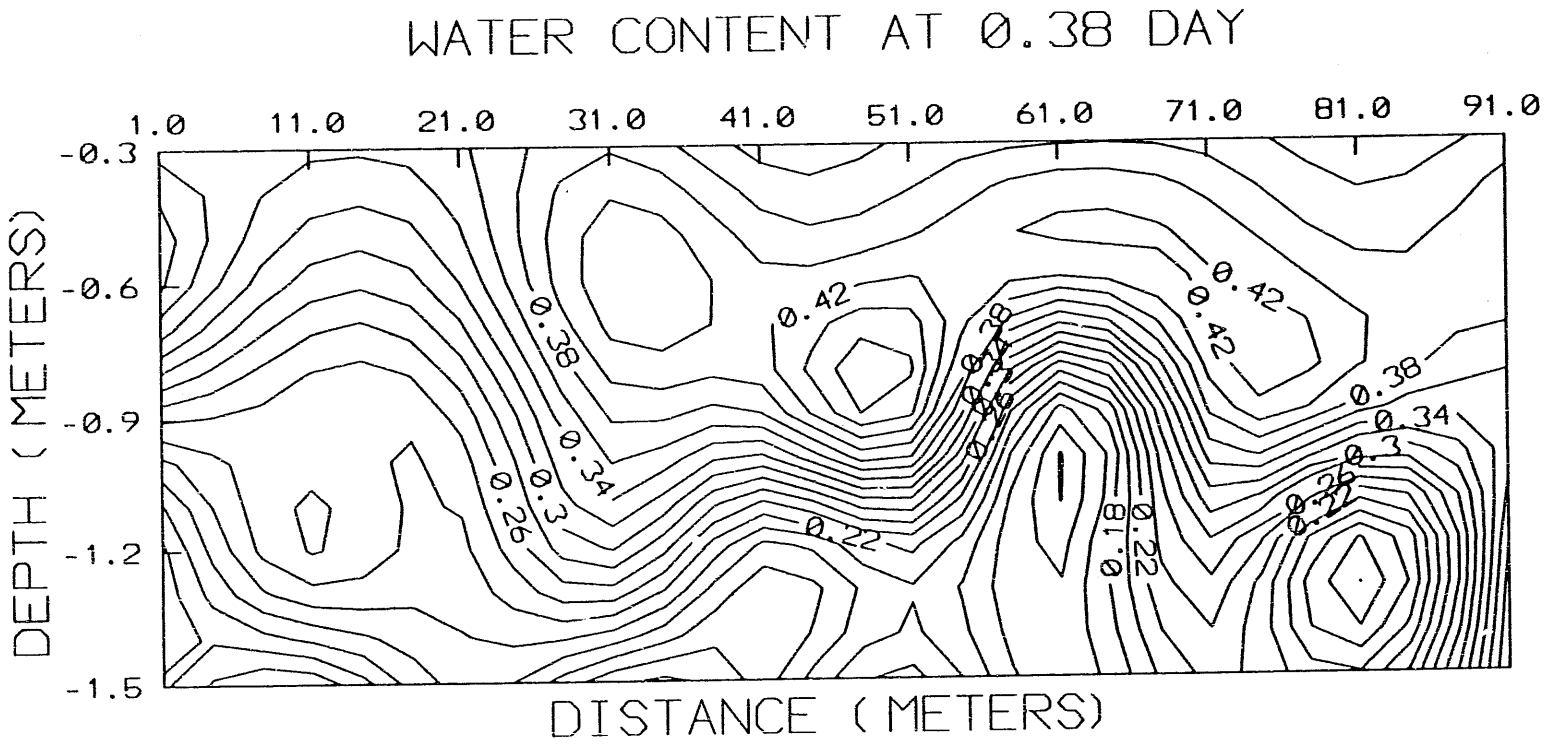
WATER CONTENT AT 0.38 DAY
1.0
11.0
21.0
31.0
41.0
51.0
61.0
71.0
81.0
91.0
-0.3
-0.6
-0.9
-1.2
-1.5
DEPTH (METERS)
DISTANCE (METERS)
0.42
0.38
0.34
0.3
0.26
0.22
0.18

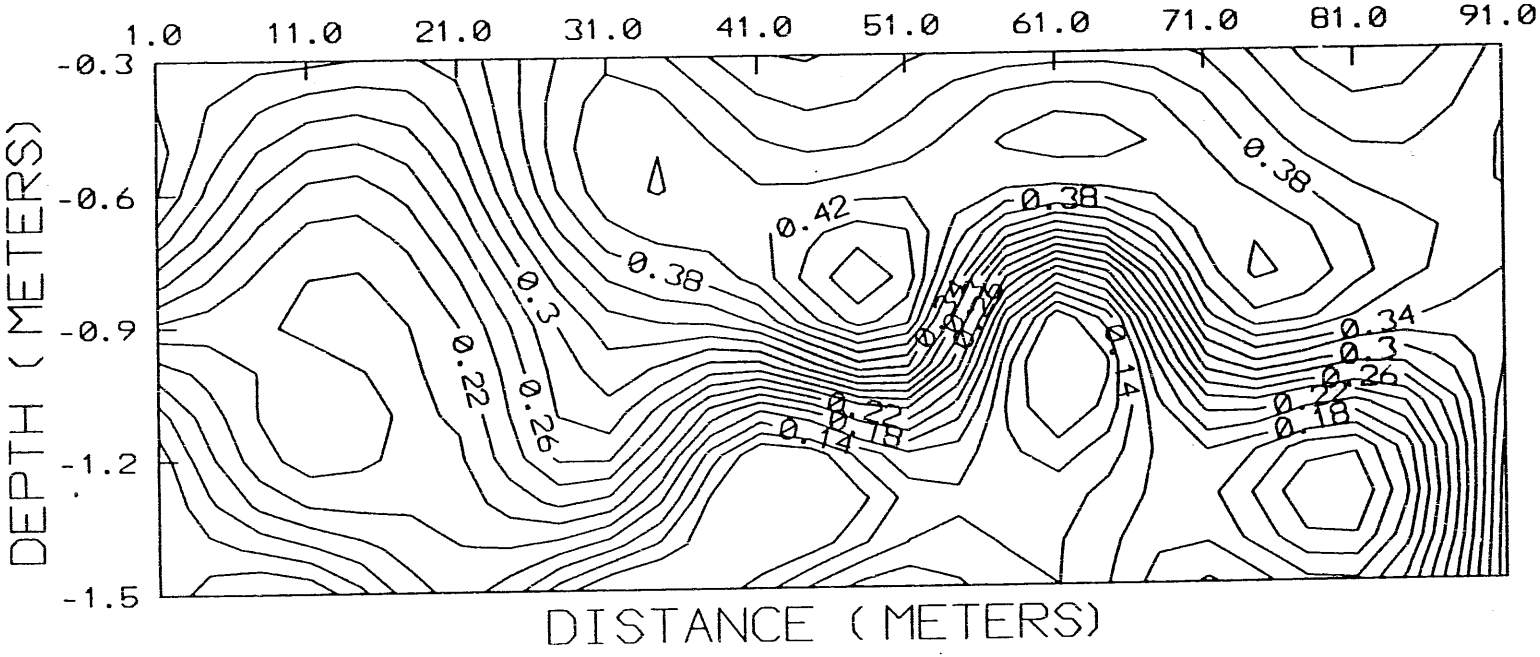
WATER CONTENT AT 11.25 DAYS
1.0
11.0
21.0
31.0
41.0
51.0
61.0
71.0
81.0
91.0
-0.3
-0.6
-0.9
-1.2
-1.5
DEPTH (METERS)
DISTANCE (METERS)
0.42
0.38
0.38
0.38
0.34
0.3
0.3
0.26
0.26
0.22
0.22
0.18
0.18
0.14
0.14

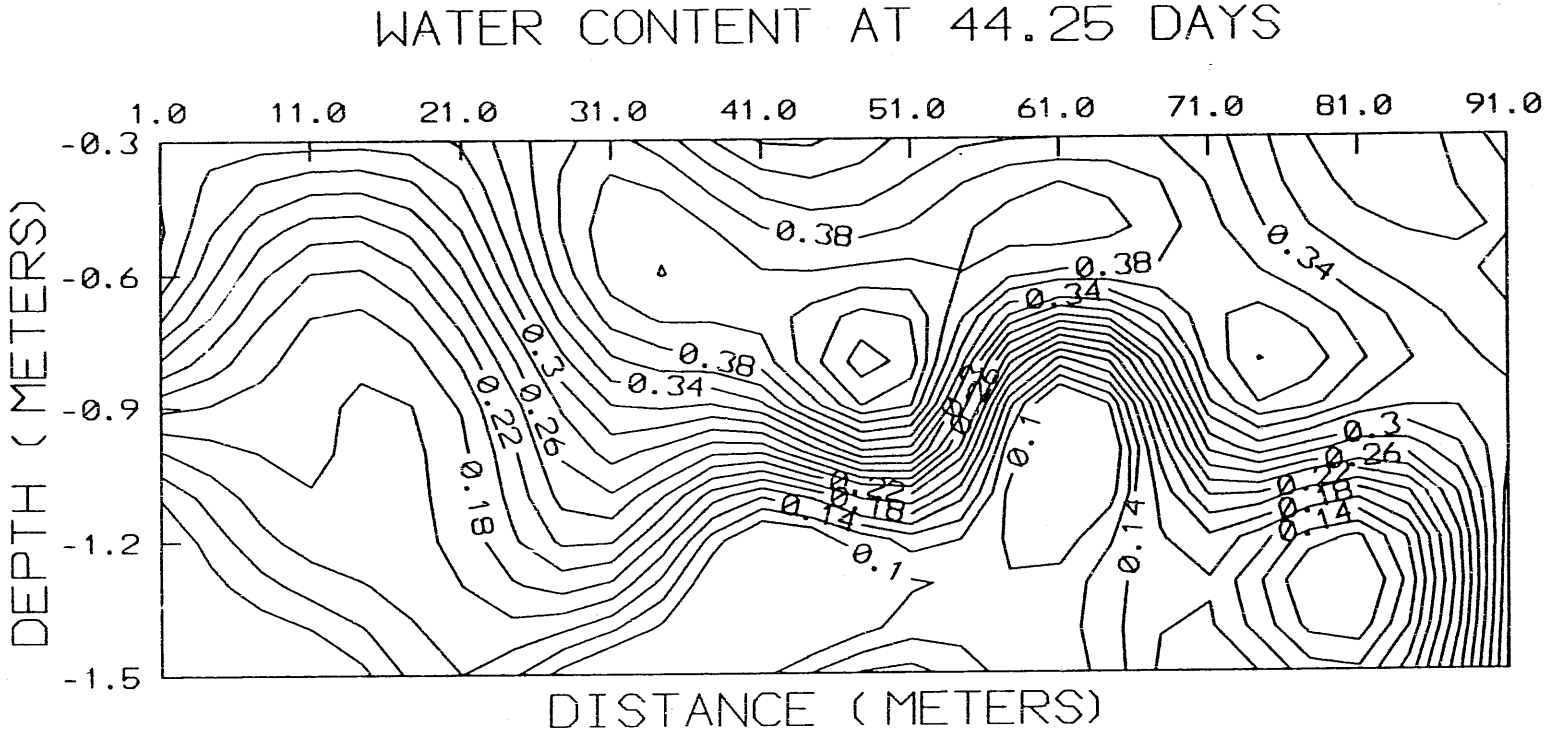
WATER CONTENT AT 44.25 DAYS
1.0
11.0
21.0
31.0
41.0
51.0
61.0
71.0
81.0
91.0
-0.3
-0.6
-0.9
-1.2
-1.5
DEPTH (METERS)
DISTANCE (METERS)
0.38
0.34
0.3
0.26
0.22
0.18
0.14
0.1

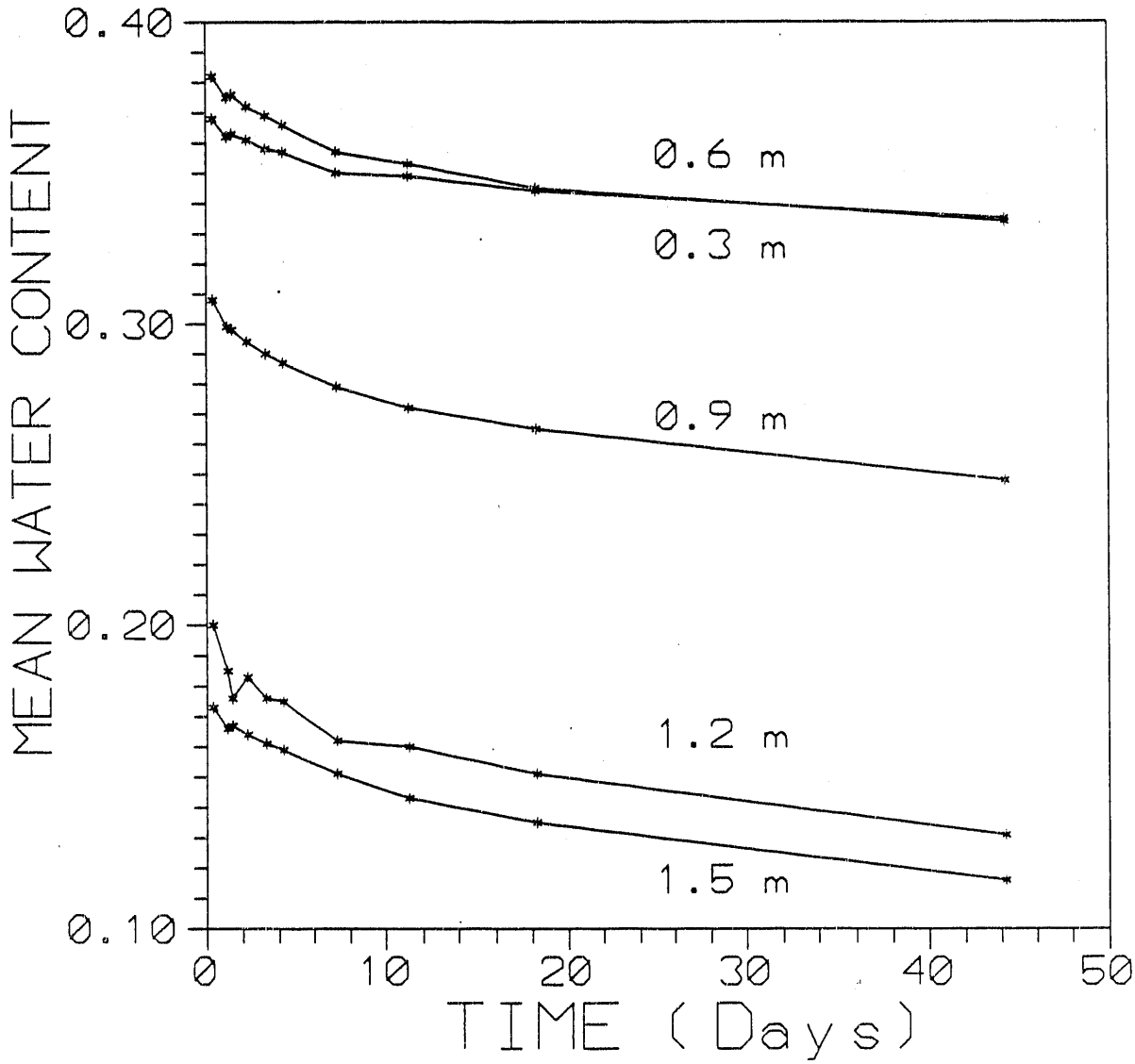
0.40
0.30
0.20
0.10
MEAN WATER CONTENT
0.6 m
0.3 m
0.9 m
1.2 m
1.5 m
0
10
20
30
40
50
TIME (Days)

Fig 6

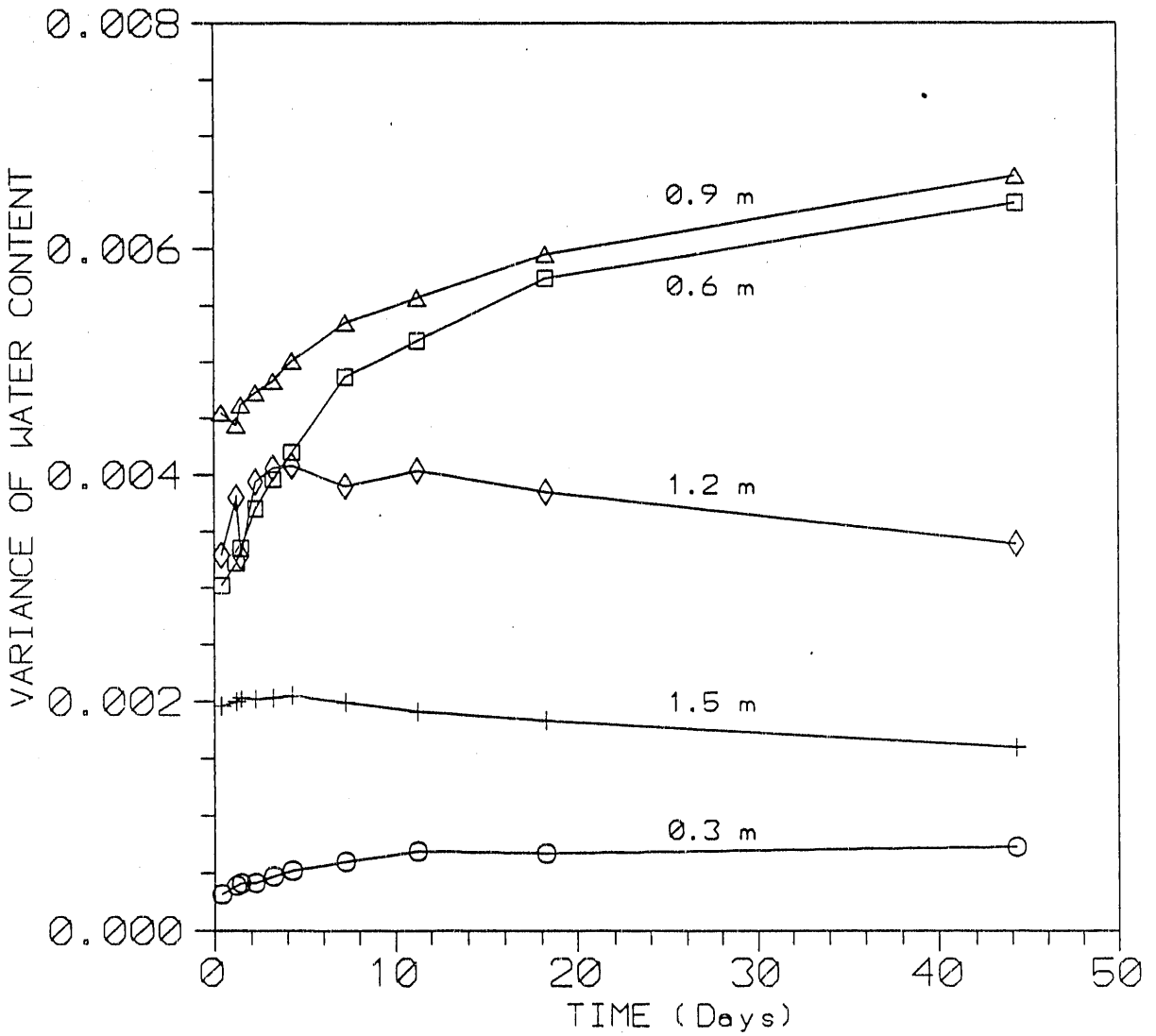
0.008
0.006
0.004
0.002
0.000
VARIANCE OF WATER CONTENT
0.9 m
0.6 m
1.2 m
1.5 m
0.3 m
0
10
20
30
40
50
TIME (Days)

Fig 5

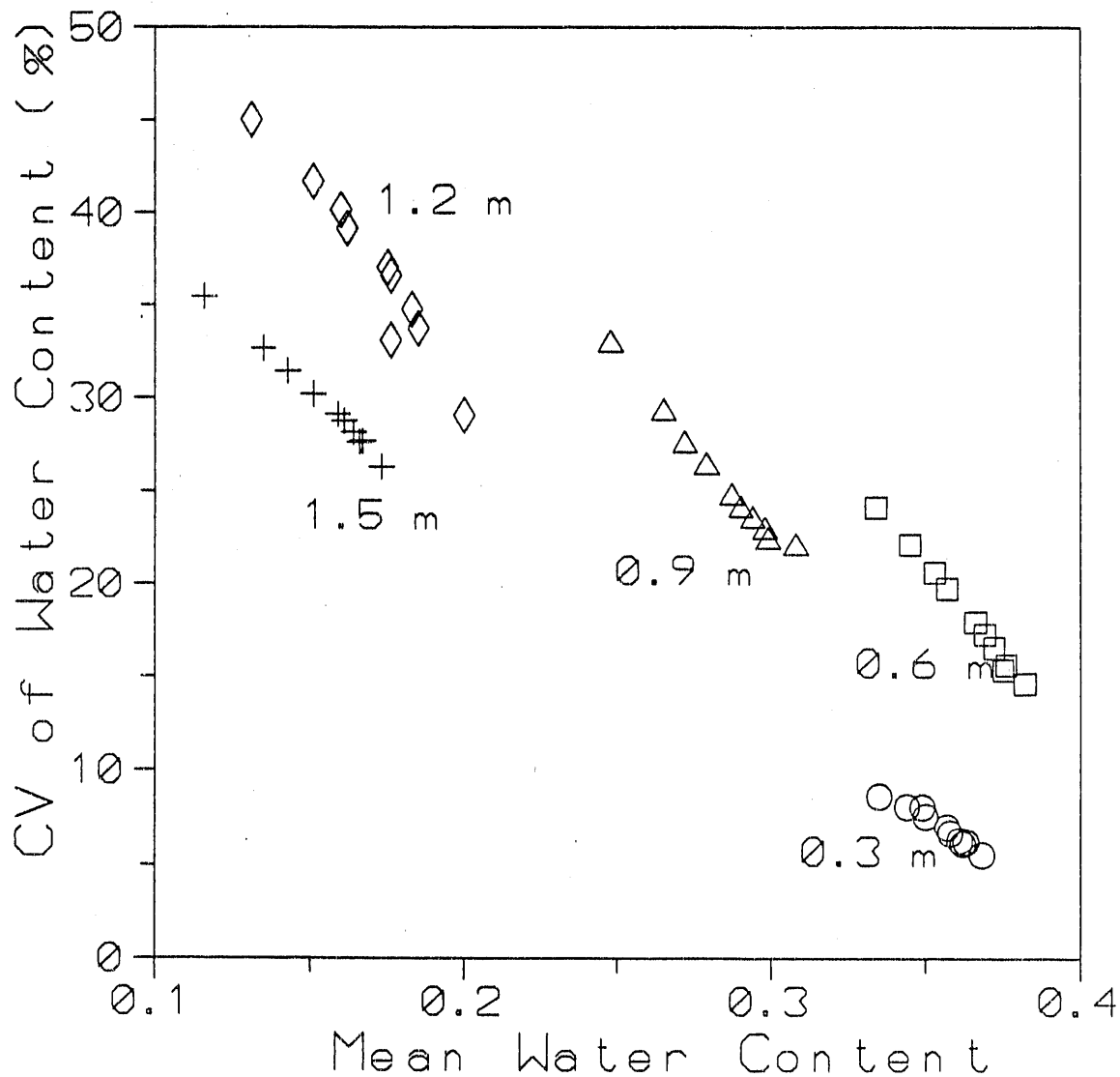
CV of Water Content (%)
50
40
30
20
10
0
0.1
0.2
0.3
0.4
Mean Water Content
1.2 m
1.5 m
0.9 m
0.6 m
0.3 m

Fig

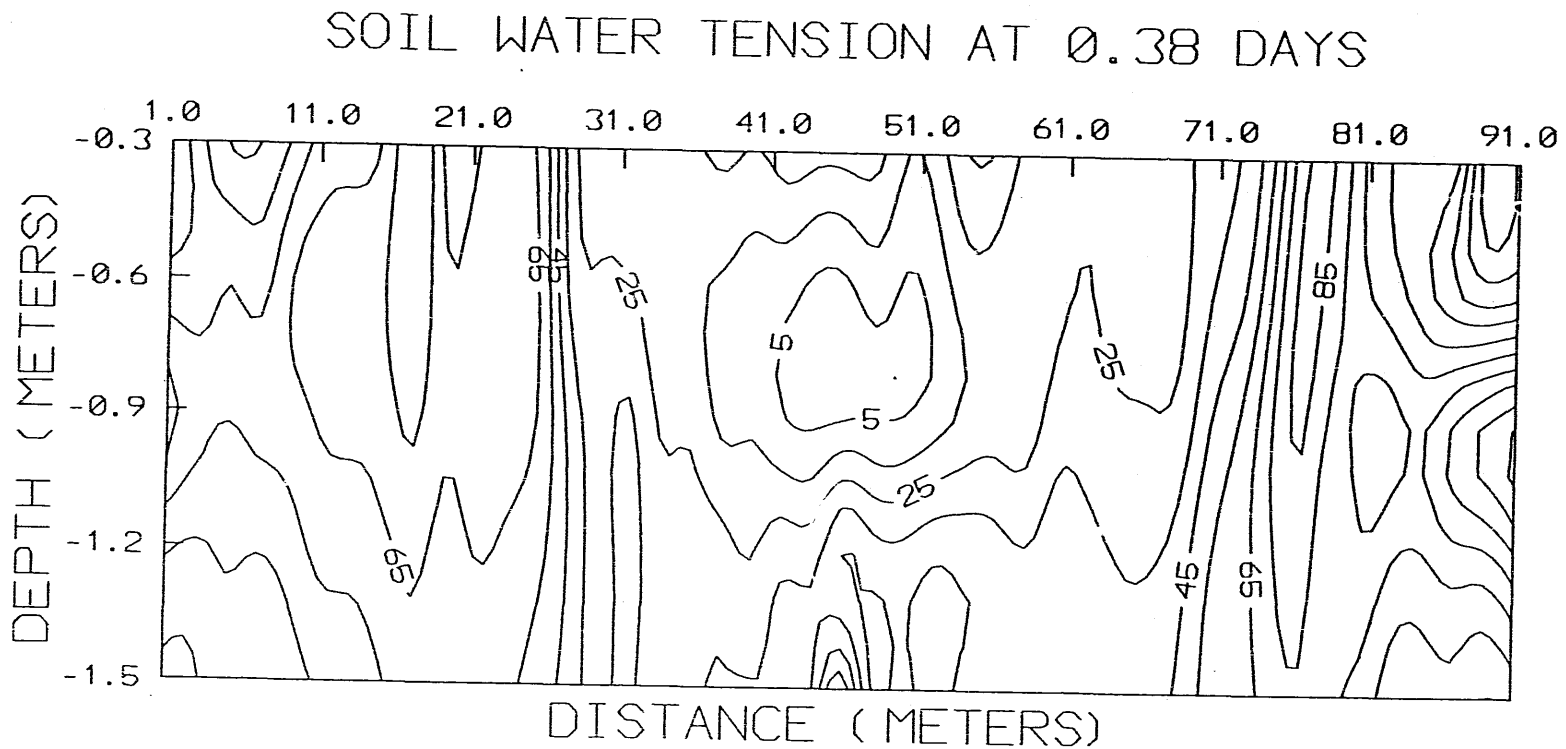
SOIL WATER TENSION AT 0.38 DAYS
1.0
11.0
21.0
31.0
41.0
51.0
61.0
71.0
81.0
91.0
-0.3
-0.6
-0.9
-1.2
-1.5
DEPTH (METERS)
DISTANCE (METERS)
65
45
25
5
5
25
25
65
45
65
85

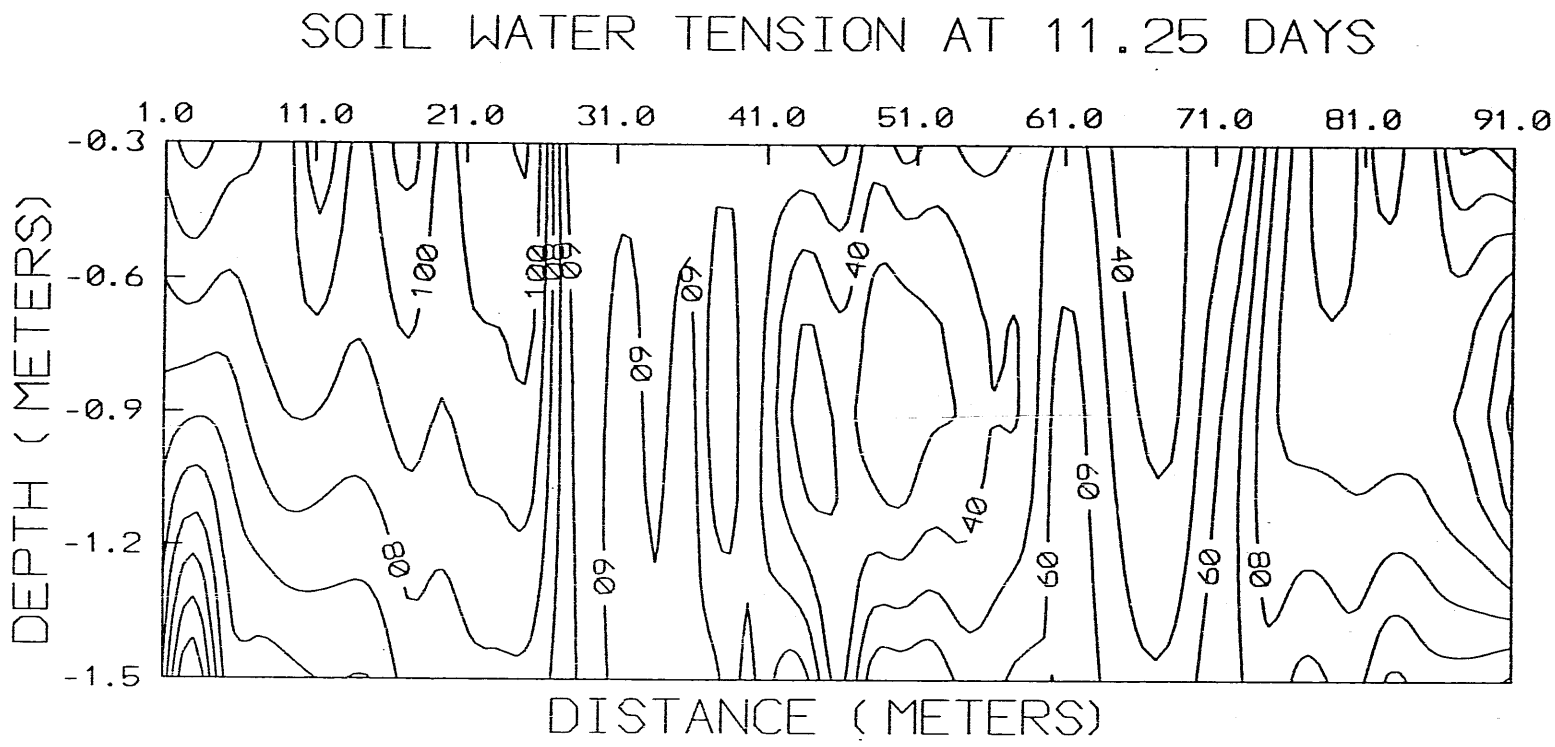
SOIL WATER TENSION AT 11.25 DAYS
1.0
11.0
21.0
31.0
41.0
51.0
61.0
71.0
81.0
91.0
-0.3
-0.6
-0.9
-1.2
-1.5
DEPTH (METERS)
DISTANCE (METERS)
100
100
100
80
60
60
60
40
40
40
60
60
60
80

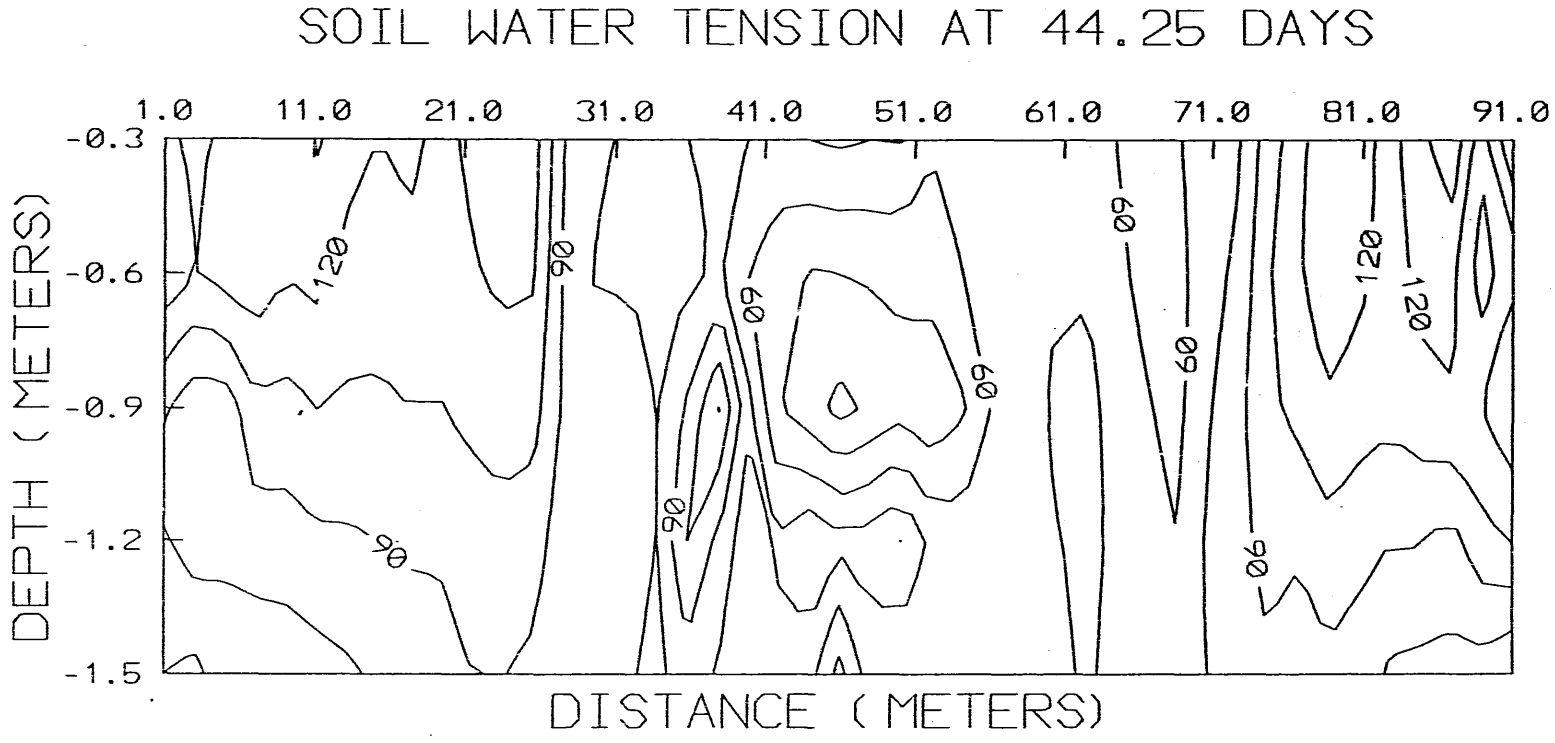
SOIL WATER TENSION AT 44.25 DAYS
1.0
11.0
21.0
31.0
41.0
51.0
61.0
71.0
81.0
91.0
-0.3
-0.6
-0.9
-1.2
-1.5
DEPTH (METERS)
DISTANCE (METERS)
120
90
60
120
90
60
90
60
120
90
60

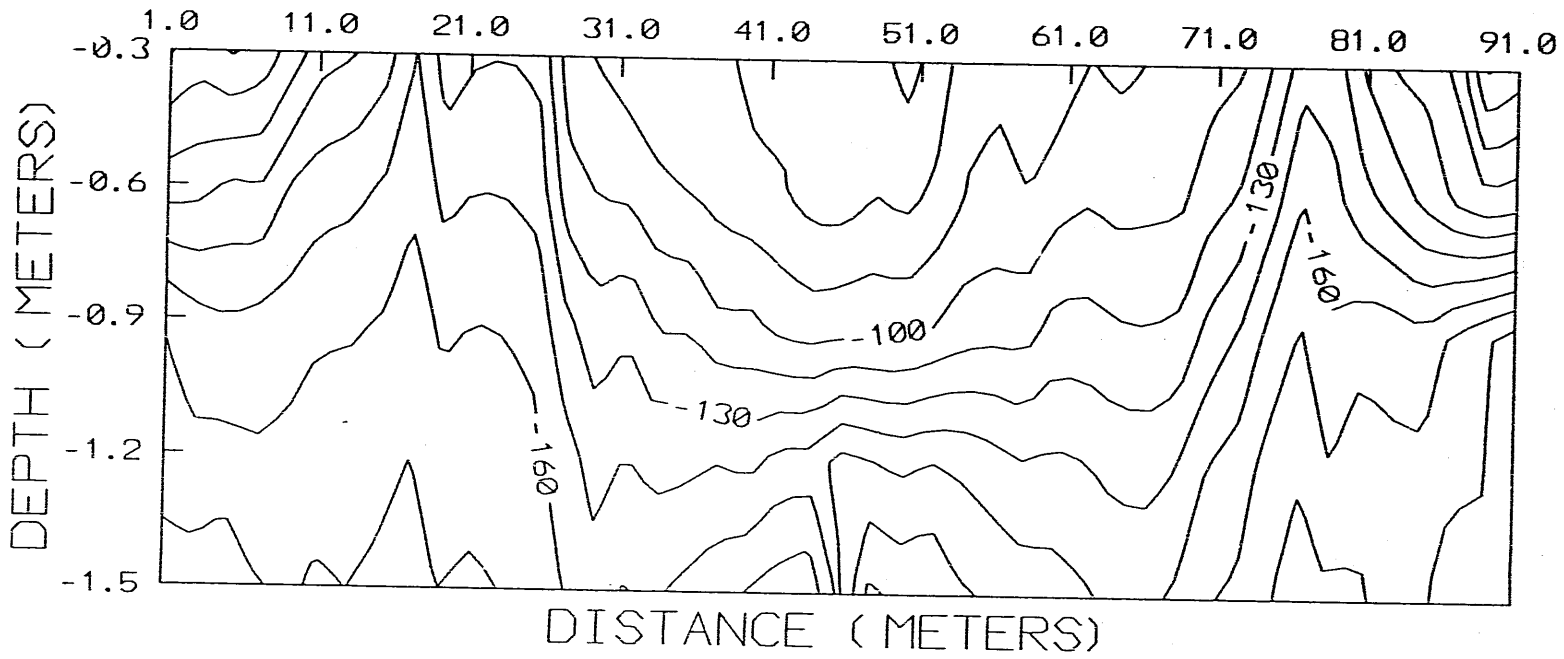
TOTAL HEAD AT 0.38 DAYS
1.0
11.0
21.0
31.0
41.0
51.0
61.0
71.0
81.0
91.0
-0.3
-0.6
-0.9
-1.2
-1.5
DEPTH (METERS)
-100
-130
-160
-130
-160
DISTANCE (METERS)

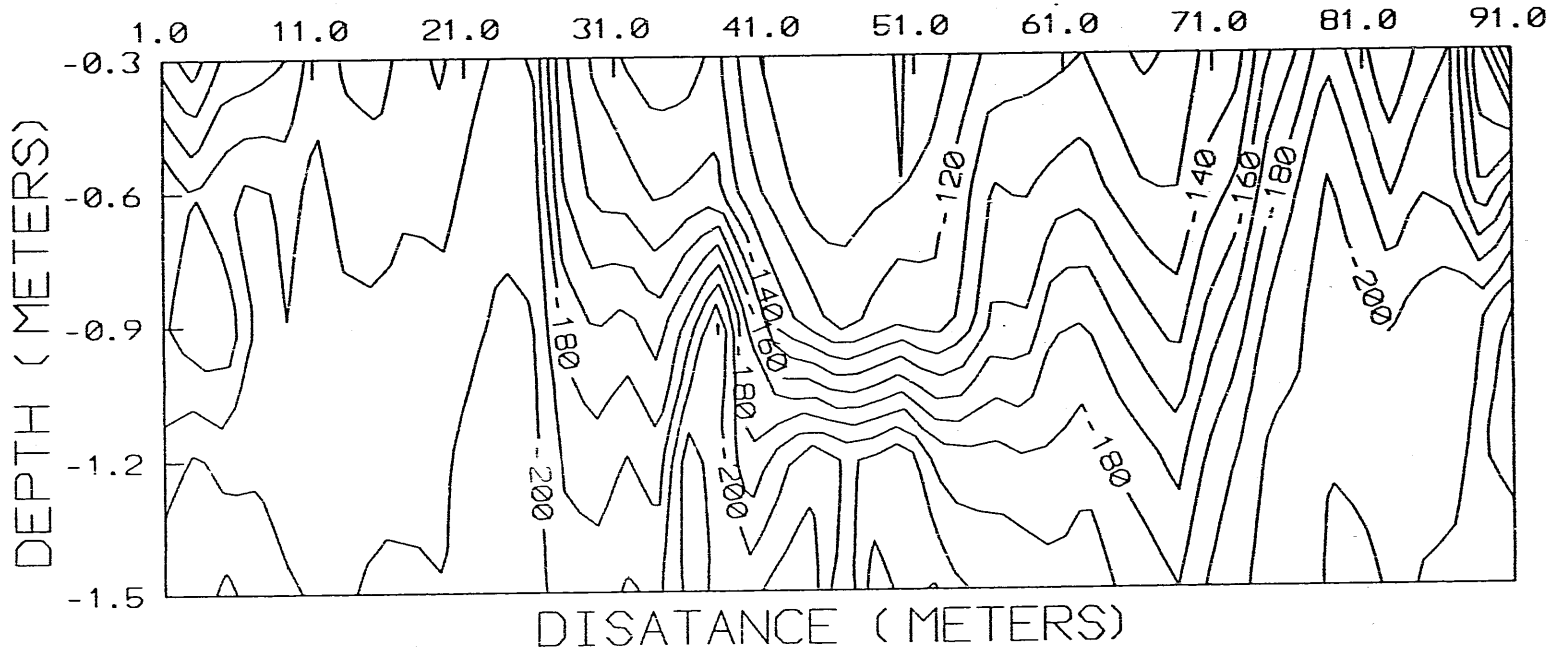
TOTAL HEAD AT 44.25 DAYS
1.0
11.0
21.0
31.0
41.0
51.0
61.0
71.0
81.0
91.0
-0.3
-0.6
-0.9
-1.2
-1.5
DEPTH (METERS)
DISATANCE (METERS)
120
140
160
180
200

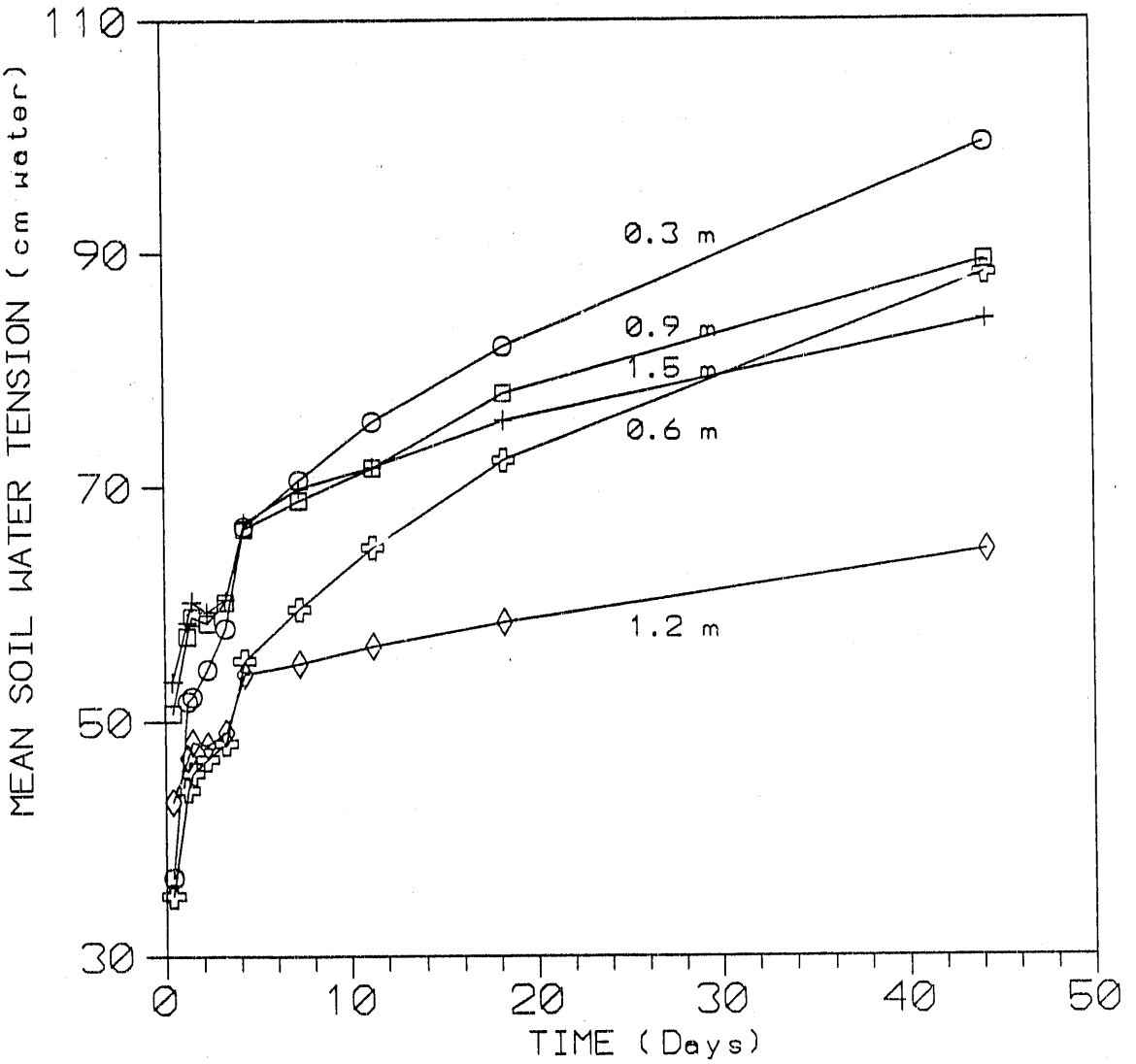
MEAN SOIL WATER TENSION (cm water)
110
90
70
50
30
0
10
20
30
40
50
TIME (Days)
0.3 m
0.9 m
1.5 m
0.6 m
1.2 m

Fig 9

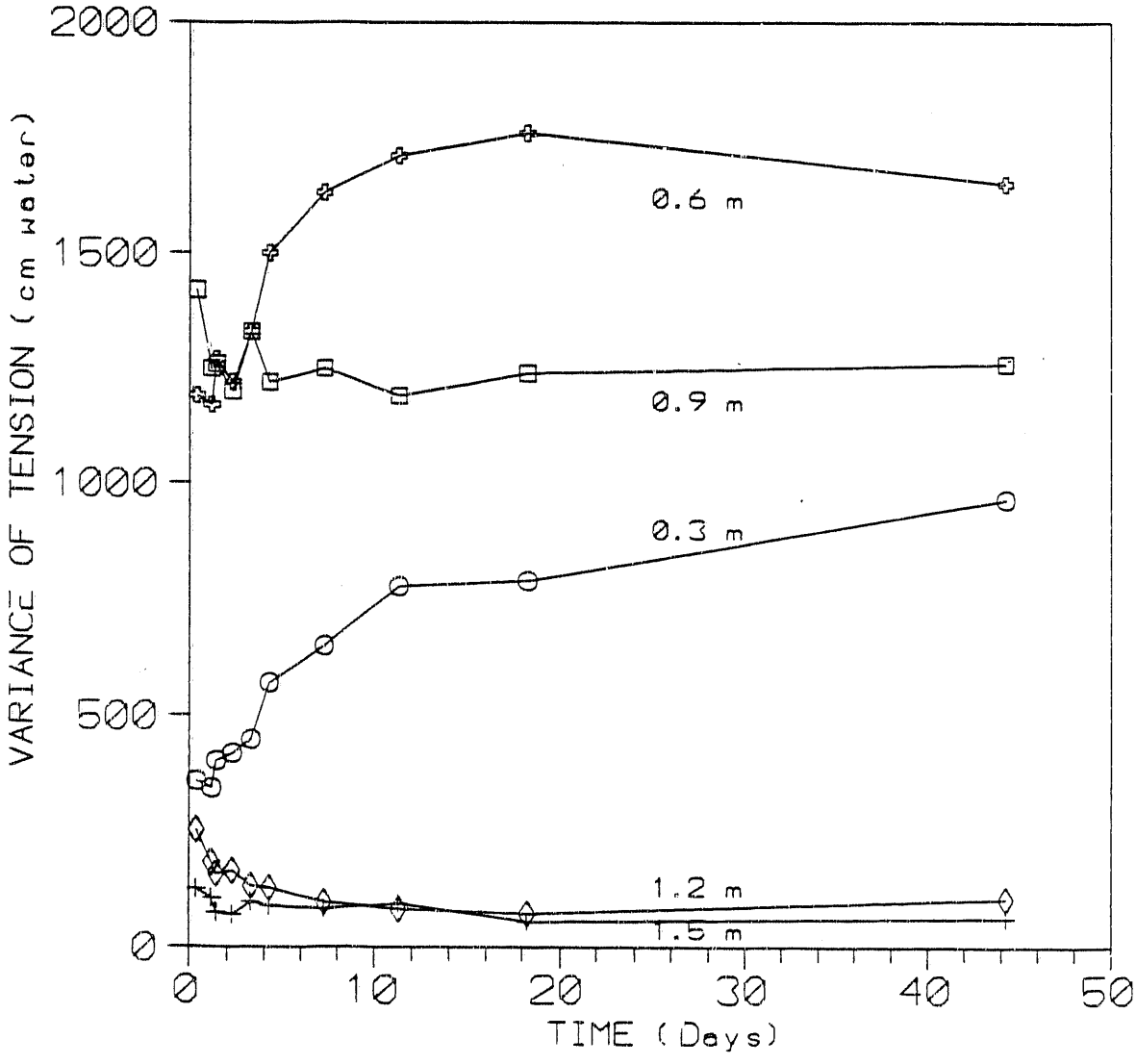
2000
1500
1000
500
0
VARIANCE OF TENSION (cm water)
0.6 m
0.9 m
0.3 m
1.2 m
1.5 m
0
10
20
30
40
50
TIME (Days)

Fig 10

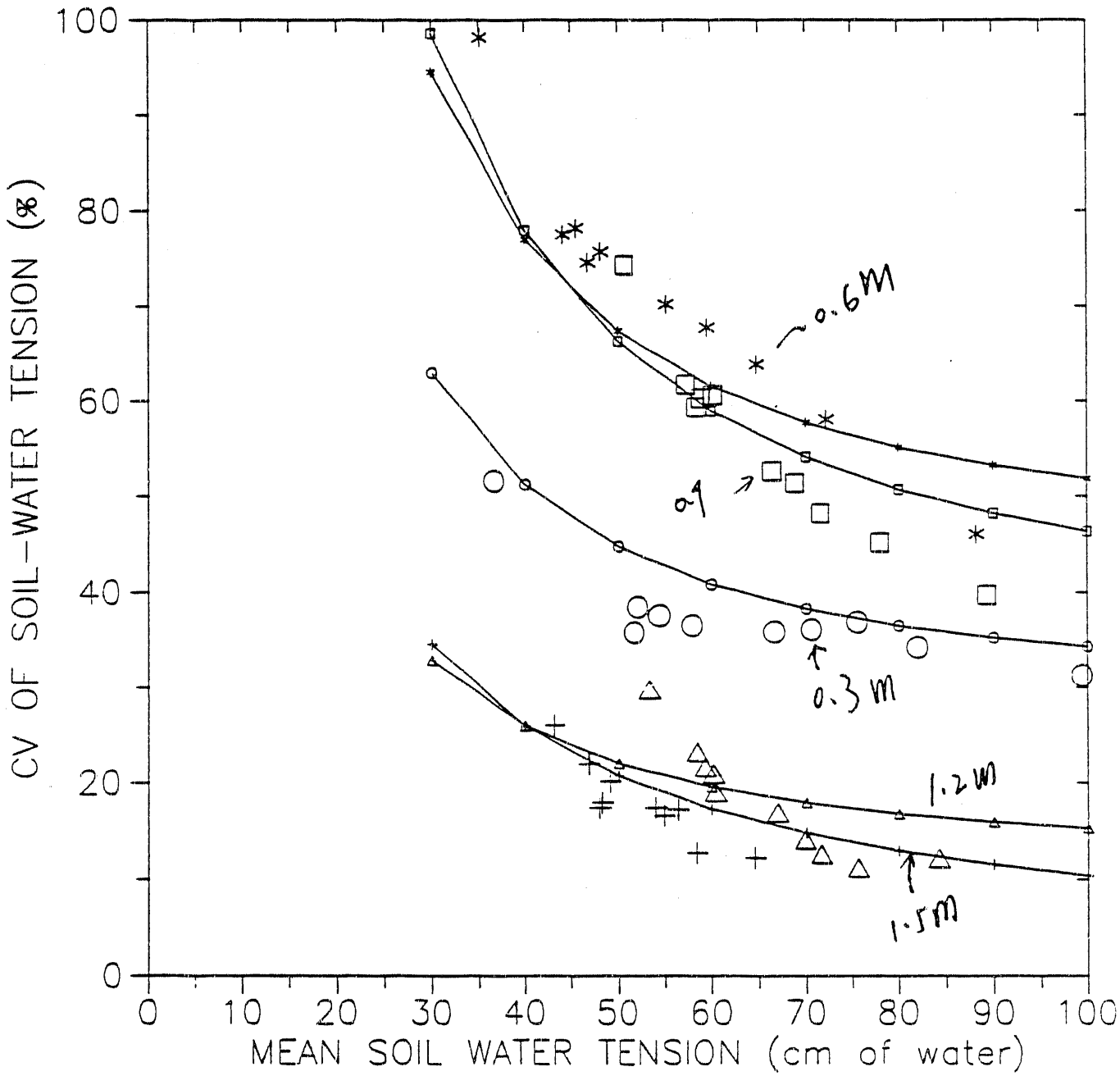
CV OF SOIL-WATER TENSION (%)
MEAN SOIL WATER TENSION (cm of water)
0
20
40
60
80
100
0
10
20
30
40
50
60
70
80
90
100
0.6m
0.9
0.3m
1.2m
1.5m

Fig 11

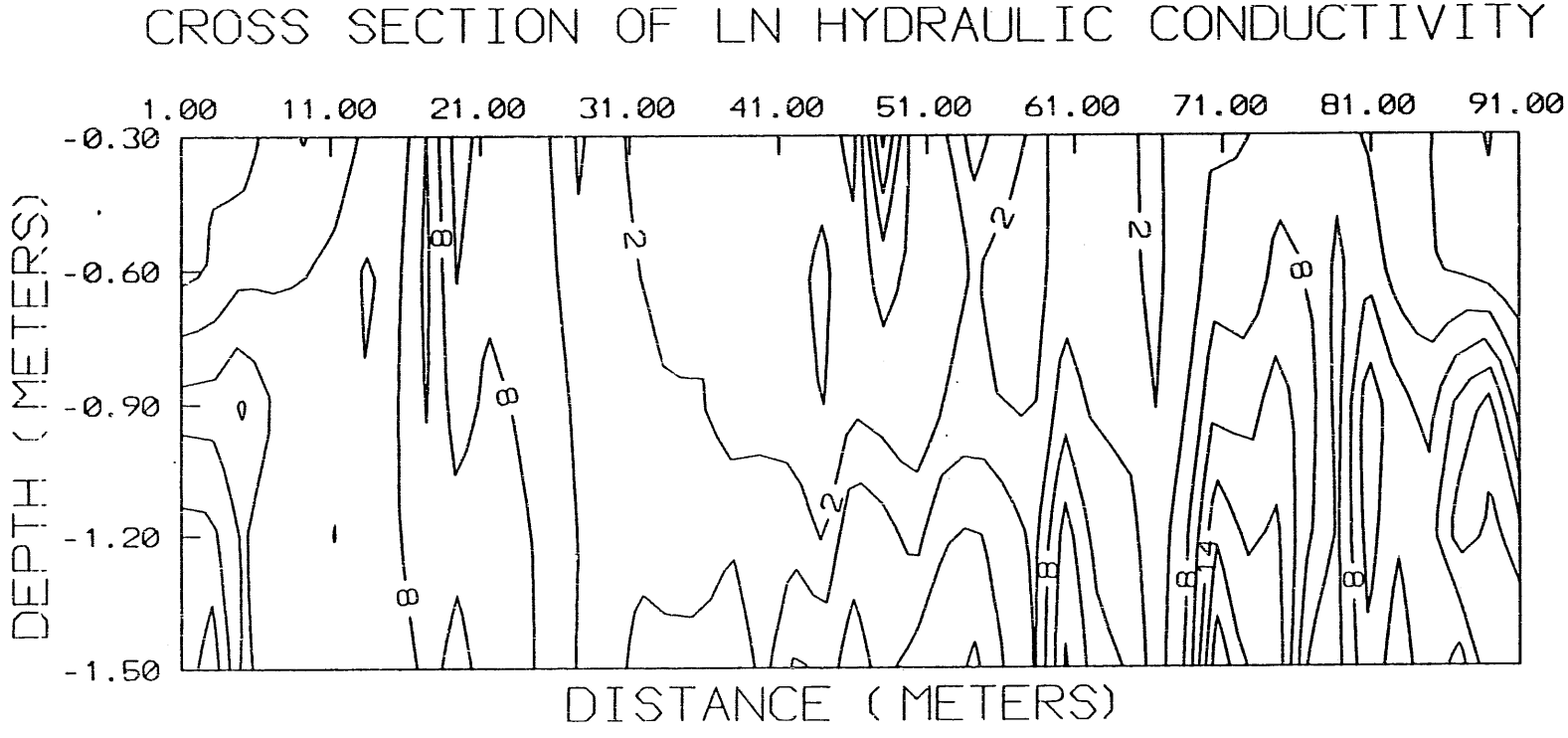
CROSS SECTION OF LN HYDRAULIC CONDUCTIVITY
1.00
11.00
21.00
31.00
41.00
51.00
61.00
71.00
81.00
91.00
-0.30
-0.60
-0.90
-1.20
-1.50
DEPTH (METERS)
DISTANCE (METERS)
8
2
0
4

CROSS SECTION OF PORE SIZE DISTRIBUTION PARAMETERS

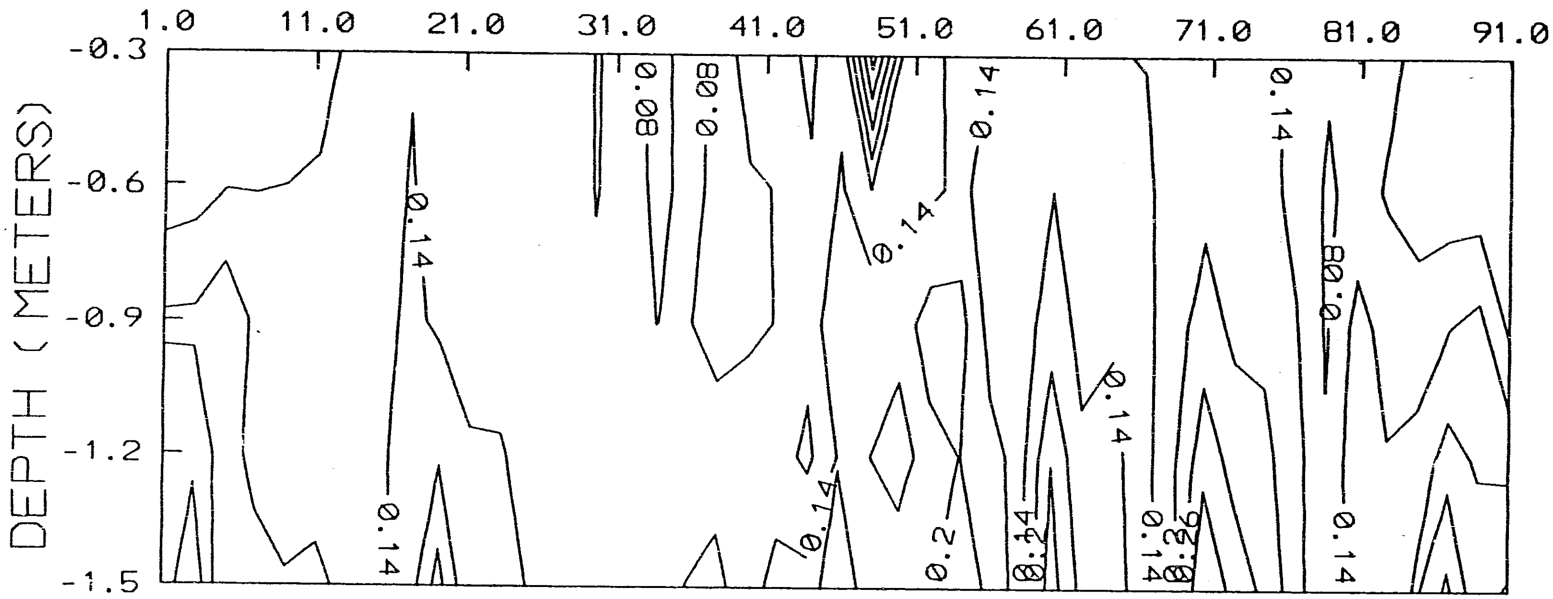

DISTANCE (METERS)

Fig12b

END

DATE
FILMED
4 / 29 / 92